

# Minimum Test Effort-based Derivation of Constant-Fatigue-Life curves - displayed for the brittle UD composite materials - **DRAFT**

Prof. Dr.-Ing. habil. Ralf Cuntze VDI, Ralf\_Cuntze@t-online.de, 0049 8136 7754

Affiliation: Retired from industry, MAN-Technologie, Augsburg, Germany

**Keywords:** *Constant-fatigue-life modeling, composites, failure criteria*

## **Abstract:**

Series production of safety-relevant structural parts requires a Design Verification guaranteeing Structural Integrity. This means, it is to demonstrate that “No relevant limit failure state is met considering all Dimensioning Load Cases (DLCs)”. These DLCs involve static, dynamic, and cyclic loading focusing lifetime. However, lifetime prediction is a pain point for a better use especially of laminated composites in lightweight design. A generally practical tool is not available. Hence, each novel high-performance UD-lamina-composed laminate requires a new effortful test campaign. Therefore, the idea of the author-founded Germany-wide group BeNa (in 2010) was to base fatigue life prediction ‘embedded and lamina-wise’ in order to become more general in future. This idea also fits to the authors ‘modal’ Failure-Mode-Concept, which is based on material symmetry facts which dedicates a ‘generic’ number to *ideally homogeneous* materials, namely 2 for isotropic material and 5 for the transversely-isotropic UD lamina. Fracture morphology gives evidence: Each strength property corresponds to a distinct strength failure mode or a distinct strength failure type, to Normal Fracture (NF) or to Shear Fracture (SF). In the case of UD materials 2 FiberFailure and 3 InterFiberFailure (IFF) modes are faced.

In lifetime prediction *strain-life* and *stress-life* models are used. For ductile materials one single plastic strain-linked yield mechanism dominates and *strain-life* models are applied. However for brittle materials the elastic strain becomes dominant and stress-life models are applied. Micro-damage mechanisms drive fatigue failure and different fracture mechanisms come to act. This asks for a modal approach that captures all fracture failure modes.

The automatic establishment of the not piecewise straight Constant Fatigue Life (CFL) curves is the challenging task. All SN-curves’ information and all the CFL curves ( $N = \text{const}$ ) are captured by the Haigh Diagram  $\sigma_a(\sigma_m)$ , with  $\sigma_a$  the stress amplitude and  $\sigma_m$  the mean stress.

Author’s idea for the generation of the ‘Automatic’ SFC-curve is to provide: (1) At minimum one single SN-curve as Master curve of each mode (*by measurement*). (2) Failure criterion that can quantify the micro-damage portions under cyclic loading (*due to experience given by the static one*). (3) A model that can predict other SN-curves on the basis of a mode Master Curve (*by Kawai’s Model ‘Modified Fatigue Strength Ratio  $\Psi$ ’*). (4) A physical model to map the test data in the transition domain as *most problematic region in the Haigh diagram*, where the modes interact and the CFL curve heavily decays (*decay function was found*).

A first model validation of this private investigation with test data from Dr. C. Hahne, AUDI, looks very promising and asks for funding.

1	Introduction .....	3
1.1	Fatigue Design Verification (DV) Task with Terms .....	3
1.2	Fatigue Micro-Damage Drivers of Ductile and Brittle behaving Materials .....	4
1.3	State-of-the-Art considering Cyclic strength of UD ply-composed Laminates .....	5
1.4	Constant amplitude loading and variable amplitude loading .....	6
1.5	Definition SN-curve and Fatigue-driving Equivalent Stress .....	6
1.6	Proportional and non-proportional loading (stressing) and mean stress sensitivity .....	7
2	Modeling of SN-curves in the Three Fatigue Domains and appropriate Choice .....	8
2.1	Modeling of SN-curves .....	8
2.1.1	General Modeling of SN-curves .....	8
2.1.2	Modeling final HCF-domain with VHCF .....	8
2.2	Relation of the Material Stressing Effort Eff with the Micro-damage D .....	9
2.3	Statistical properties in Design Verification (DV) .....	10
3	Failure-Mode-Concept (FMC) and static Strength Failure Criteria (SFC) .....	12
3.1	Features of the Failure-Mode-Concept .....	12
3.2	Modal and Global SFCs .....	14
3.3	FMC-based Failure Modes, SFCs and SFC-visualization .....	15
3.4	Application of the Static UD-SFCs to determine Cyclic micro-damage Portions .....	19
4	FMC-based Constant-Fatigue-Life Estimation Model for UD-ply-composed Laminates .....	20
4.1	Idea of an Automatic Establishment of Constant Fatigue Life Curves .....	20
4.2	SN curves, derived with Kawai's Model 'Modified Fatigue Strength Ratio $\Psi$ ' .....	21
4.3	Derivation of Constant Fatigue Life CFL curves in the Transition Domain .....	24
5	Complete CFL-curve Model using the Decay Functions $f_d$ in the Haigh-Diagram .....	28
5.1	Derivation of the Full Procedure .....	28
5.2	CFL curves, applying the Mode Decay Functions $f_d$ in various UD Haigh-Diagrams .....	31
5.3	Steps of the FMC-based Fatigue Life Estimation Procedure .....	36
6	Conclusions on the Elaborated Novel Ideas .....	39

# 1 Introduction

## 1.1 Fatigue Design Verification (DV) Task with Terms

Generally, in design verification it is to demonstrate that “No relevant limit failure state is met considering all Dimensioning Load Cases (DLCs)”. This involves static DLCs, dynamic DLCs and cyclic ones, with the focus lifetime. Addressed are Design Dimensioning and Design Verification (DV). Focused in design is the strength DV of non-cracked structural parts and the fracture mechanics-based DV of cracked structural parts by Damage Tolerance Tools, see [1]. The size of the damage decides whether it is to apply a SFC with  $F = 1$  for Onset-of-fracture in a critical material ‘Hot Spot’ of the un-cracked (*probably still micro-damaged*) structural part or a fracture mechanics-based Damage Tolerance Condition in case of a technical crack (*macro-damaged*). Estimation of lifetime means to assess the growth of the micro-damage before reaching a technical crack size.

Domains of Fatigue Scenarios and Analyses are:

LCF: high stressing and straining

HCF: intermediate stressing  $10.000 < n < 2.000.000$  cycles (*rotor tubes, bridges, towers, off-shore structures, planes, etc.*)

VHCF: low stress and low strain amplitudes (*see SPP1466 Very High Cycle Fatigue > 10<sup>7</sup> cycles, in centrifuges, wind energy rotor blades, etc.*).

Design Verification demands for reliable reserve factors  $RF$  which demand for reliable SFCs. Such a SFC is the mathematical formulation  $F = 1$  of a failure curve or of a failure surface (body). Generally required are a yield condition and fracture strength conditions. A yield SFC usually describes just one mode, i.e. for isotropic materials the classical ‘Mises’ describes shear yielding SY. Fracture SFCs for isotropic materials usually have to describe two independent fracture modes, shear fracture SF and normal fracture NF. For the here focused transversely-isotropic uni-directionally reinforced UD- laminas one counts five [1, 2, 3, 4, 5].

Principally, in order to avoid either to be too conservative or too un-conservative, a separation is required of the always needed ‘analysis of the average structural behavior’ in Design Dimensioning (*using average properties and average stress-strain curves*) in order to obtain best information (= 50% expectation value) from the mandatory single Design Verification analysis of the final design, where statistically minimum values for strength and minimum, mean or maximum values for other task-demanded properties are applied as Design Values.

Cyclic fatigue Life consists of three phases. This means for a laminate [1,6]:

Phase I: Increasing micro-damage acts in a lamina embedded in a laminate up to a discrete micro-damage onset. Determination of accumulating micro-damage portions (Schädigungen) initiated at the end of the elastic domain and dominated by diffuse micro-cracking + matrix yielding inclusively cavitation under 3D-tensile stressing, and finally little cracks such as micro-delaminations. Degradation begins with the onset of the diffuse micro-cracking in the strain hardening domain until Inter-Fiber-Failure (IFF1, IFF3) occurs.

Phase II: Stable local discrete micro-damage growth within the laminate up to the growth of the width of the dominating discrete micro-cracks (*after localization*) incl. micro-delaminations. In cyclic loading, degradation is more diffuse than in static loading. Phase II is usually dedicated to fatigue and basically linked to discrete micro-damage growth

Phase III: Final in-stable fracture of laminate initiated by Fiber-Failure (FF) and probably the compressive IFF2 of any lamina and possible criticality of the loaded laminate due to the macro-damage delamination. This phase is usually dedicated to fracture mechanics, to macro-damage and macro-cracking.

Methods for the prediction of durability (Dauerhaftigkeit), regarding the lifespan of the structural material and thereby of the structural part, involves long time static loading which is linked to ‘static Fatigue‘(→Dauer-Standfestigkeit) and further (cyclic) fatigue (→Dauer-Schwingfestigkeit ≡ Dauer-Festigkeit). Fatigue failure requires a Procedure for Fatigue Life Estimation necessary to perform the cyclic DV.

## ***1.2 Fatigue Micro-Damage Drivers of Ductile and Brittle behaving Materials***

There are strain-life (*plastic deformation decisive*) and *stress-life* models used. For ductile materials strain-life (*plastic strain-based*) models are applied because a single yield mechanism dominates. For brittle materials the elastic strain amplitude becomes dominant and stress-life models are applied. With brittle materials inelastic micro-damage mechanisms drive fatigue failure and several fracture mechanisms may come to act. This asks for a modal approach that captures all failure modes which are here fracture modes. In this context shall is stated below

Above two models can be depicted in a Goodman diagram and in a Haigh diagram. The Goodman diagram provides the maximum tolerable stresses  $\sigma_{\max}$  of the material (*it is commonly used in construction specifically for concrete*). The Haigh diagram ( $\sigma_a, \sigma_m$ ) will be applied here because in general just to use  $\sigma_a$  or  $\Delta\sigma = 2 \cdot \sigma_a$  or  $\sigma_{\max}$  is not sufficient for the analysis. A Haigh Diagram represents all available SN curve information by its ‘Constant Fatigue Life (CFL) curves, the focus of this investigation.

Basic differences between ductile and brittle materials are to consider [1, 3]:

- Ductile Material Behavior, isotropic materials: mild steel
  - 1 *micro-damage* mechanism acts ≡ “*slip band shear yielding*“ and drives micro-damage

under tensile, compressive, shear and torsional cyclic stresses: *This single mechanism is primarily described by 1 SFC, a yield failure condition (HMH, 'Mises' )!*

- Brittle Material Behavior, isotropic materials: concrete, grey cast iron, etc.  
*2 micro-damage driving mechanisms act  $\equiv$  2 fracture failure modes Normal Fracture failure (NF) and Shear Fracture failure (SF) under compression described by 2 fracture conditions, the 2 SFCs for NF and SF, where porosity is always to consider*
- Brittle Material Behavior, transversely-isotropic UD-materials:  
*5 micro-damage driving fracture failure mechanisms act  $\equiv$  5 fracture failure modes described by 5 SFCs or strength fracture failure conditions.*

### 1.3 State-of-the-Art considering Cyclic strength of UD ply-composed Laminates

- Experience with composites of fiber-reinforced plastics FRP monitors: These behave brittle, experience early fatigue damage, but show benign fatigue failure behavior in case of 'well-designed' laminates until finally a pretty 'Sudden Death' occurs (*fiber-dominated laminates are used in high performance stress applications whereby fiber-dominated means that there are  $0^\circ$ -plies in all significant loading directions  $\rightarrow > 3$  fiber direction angles  $\alpha$* )
- No Lifetime Prediction Method is available, that is applicable to any lamina (physical ply, lamella) and UD ply-composed laminate. The procedures base on specific laminate lay-ups and therefore the test results cannot be generally applied. Embedded ply-degradation must be non-linearly considered
- Endurance strength procedures often base – as with metals – on  $\sigma_a, \sigma_m$
- Present in Mechanical Engineering as Engineering Approach: Applying a Static Design Limit Strain of  $\varepsilon < 0.3\%$  in multi-axial laminate design practically means negligible matrix-micro-cracking in the cases of  $> 3$  fiber-directions. Design experience proved: Then practically no IFF-caused fatigue danger of a laminate is given [4, 7, 8]
- Future in Mechanical Engineering: Design Limit Strain shall be increased beyond  $\varepsilon \approx 0.5\%$  (*EU-project: MAAXIMUS to better exploit UD-materials*). Then, dependent on the matrix, first filament breaks may change the early diffuse matrix micro-cracking to a discrete and more critical localized one.
- Present Engineering Approach in Civil Engineering for FRP materials and its semi-finished products such as a pultruded rod, a strand cut-out of a fiber-grid, lamella (tape) etc. In the case of a 'not predominantly static loading' the required fatigue life must be demonstrated by measured SN-curves (Stress-failure cycle  $N$ ), the given operational loading spectrum and a hypothesis for the accumulation of the micro-damages. Bounds are set by the required minimum micro-crack width of the Serviceability Limit State SLS (GZG) and deformation restrictions for instance for bridge bending. If there are only carbon-fibers used for the reinforcement (corroding steel is no problem) then the SLS micro-crack size could be increased a little for future design.

Considering the high-performance UD lamina-composed laminates the classical fatigue tests are performed on laminates. In this context the author invited German colleagues in 2000 to discuss the fatigue strength design situation during a special meeting, according to the VDI guideline 2014, sheet 3, [7]. Then, an idea of the author-founded Germany-wide group BeNa (in 2010) was, to base the fatigue life prediction ‘embedded lamina-wise’ in order to be more general in fatigue life design in the future and to save test Costs and time. Distinct laminate test specimens shall capture the interface effect of the lamina embedded in the laminate.

#### ***1.4 Constant amplitude loading and variable amplitude loading***

Cyclic loadings are most often given by an operational loading spectrum with its automatic loss of the stress-time relationship. In *Fig.1* variable amplitude loading of the structure in operation or service is displayed ending with the ‘operational fatigue life curve’ after *Gaßner*. Further depicted is the harsher ‘constant amplitude loading’. A loading spectrum-representing block-loading instead of mapping the loading spectrum by a single constant amplitude loading stands for more realistic fatigue life estimation. Good information about the loading spectrum pays off.

The more brittle the material is the more mean stress influence acts. This is why micro-damage is not anymore caused by yielding alone (1 *strength failure mode, quantified* by  $\sigma_{eq}^{Mises}$ ) but by micro-cracking which is caused by many strength fracture failure modes. Brittle materials like the transversely-isotropic UD material with its five fracture failure modes possess strong mean stress sensitivity. That requires a failure mode-linked treatment which cannot be captured by a mean stress correction as usually still performed with not fully ductile materials. See later for the example CFRP-lamina in the Haigh diagram of §5.3, where the huge effect of the mean stress sensitivity of brittle materials is demonstrated very impressively if the ‘strength ratio’ of compressive strength and tensile strength is high.

#### ***1.5 Definition SN-curve and Fatigue-driving Equivalent Stress***

The SN curve is a so-called constant amplitude curve. *Unfortunately in practice, the SN curve parameter, termed stress ratio R, is indicated by the letter R, too. The reason for this is that R is now the Ratio of  $\sigma_{min}/\sigma_{max}$ . The strengths are bias letters denoted R from strength Resistance.*

In service, a huge number of ups and downs may be given as varying stress input (*Fig.1*). Counting methods help to reduce the number of turning points in this time-domain in order to achieve a set of simple stress reversals. The rain-flow counting method from Endo-Matsuiishi, 1968, is the most often used method. The resulting load spectrum allows the application of a Miner Rule to estimate fatigue life under complex loading or stressing, respectively.

Analogous to the ductile material case where a multi-axial stress state is captured by an equivalent stress  $\sigma_{eq}^{Mises}$  for the yield mode it may be assumed that for anisotropic materials the same is valid for each single fracture mode, if equivalent stresses are available such as it is possible with the FMC-based SFCs of the author.

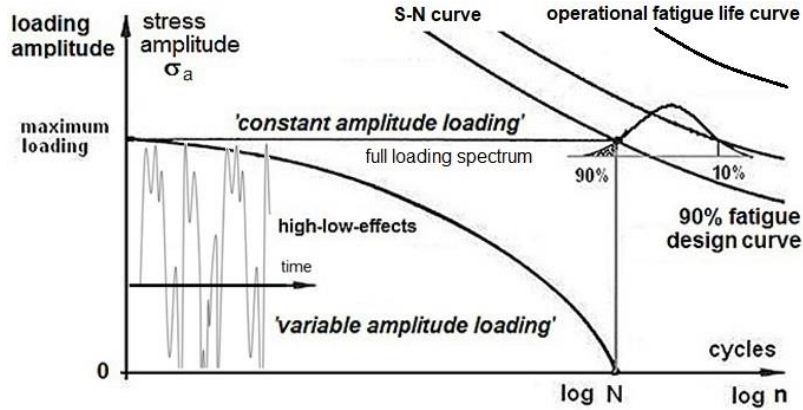


Fig.1: Display of constant amplitude loading and load history-linked variable amplitude loading

For brittle isotropic and anisotropic materials a change from uni-axial  $\sigma_a$ ,  $\sigma_{max}$  to a multi-axial, equivalent stress  $\sigma_{eq,max}^{mode}$  is welcomed and will improve the analysis.

## 1.6 Proportional and non-proportional loading (stressing) and mean stress sensitivity

### 1.6.1 Proportional and non-proportional loading

A so-called proportional loading is a concept, where all stresses are altered proportionally. Compared to proportional stressing a non-proportional stressing (*e.g. 90° out-of-phase*) may lead to a significant life reduction, at least for isotropic structural materials. Due to the time-dependent, differently oriented stress states the growing flaws may have a better chance for coalescence viewing slip bands in ductile materials under strain-controlled fatigue testing or viewing micro-cracks in brittle materials.

### 1.6.2 Mean stress sensitivity

Not fully ductile isotropic materials show an influence of the mean stress on the fatigue strength depending on the (static) tensile strength and the material type. Mean stresses in the tensile range  $\sigma_m > 0$  MPa lead to a lower permanently sustainable amplitude, whereas compressive mean stresses  $\sigma_m < 0$  MPa increase the permanently sustainable amplitude or in other words: A tensile mean stress lowers the fatigue strength and a compressive mean stress increases the fatigue strength.

## 2 Modeling of SN-curves in the Three Fatigue Domains and appropriate Choice

### 2.1 Modeling of SN-curves

#### 2.1.1 General Modeling of SN-curves

SN-curves can be modelled linearly and non-linearly in semi-log and log-log diagrams. Possible mapping formulations describe non-linear curves such as the Weibull-model and the Wearout-model [7] and linear curves in the log-log diagram. The author investigated five models mapping SN curve data, see §10.2 in [1]. The computation of the curves with its curve parameters was performed by the Mathcad code.

For brittle materials it is physically optimum to use the strength  $\bar{R}$  (*average value, marked by a bar over*) as maximum stress  $\sigma_{\max}$  at  $n = N = 1$ , being the origin of a SN-curve. This, on top, reduces the number of free parameters by one. In aerospace standards, like the HSB [8], the strength  $\bar{R}$  of not so brittle structural materials is not taken as origin in order to get more freedom for a better mapping in the domain of highest interest, namely the LCF domain. If at the end of the HCF domain a lack of data is faced, then, a so-called ‘Haibach-correction’ is often performed by halving the HCF curve-determining decay angle beyond  $n = 2 \cdot 10^6$  cycles.

#### 2.1.2 Modeling final HCF-domain with VHCF

Some materials could have an endurance limit which represents a stress level below which the material does not fail and can be cycled infinitely. If the applied stress level is below the endurance limit the material is said to have an infinite life. This might have been acceptable in some cases for the maximum HCF-level of  $2 \cdot 10^6$  cycles, however needs to be checked for VHCF because the failure mechanism might be not fully the same as for HCF. From this can be deduced that above endurance limit is an *apparent* fatigue strength.

Performing an extrapolation out of the HCF regime, for  $n > 2 \cdot 10^6$  cycles, the choice of the mapping function determines the obtained lifetime value, see the investigated SN-curve mapping models in [1]!

The choice of the SN-model mainly depends on the fact whether an endurance limit in the VHCF domain is to map or not. Such a limit seems to exist for cyclic tensioning of CFRP (*Carbon Fiber Reinforced thermoset Polymer*).

Cyclic failure always depends on the amount and distribution of flaws at the surface (*formerly often termed Weibull surface effect*) of the structural part and on those flaws within the critical material volume (*formerly often termed Weibull volume effect*). This is especially valid for the novel 3D-printed parts.



Hence, a dedication to surface-generated failure at HCF and to volume-generated failure at VHCF looks reasonable supported by novel VHCF experiments, where it became known for metals: The failure origin for VHCF changes from surface flaws, notches to internal flaws such as the different inclusion types [9]. This forced the material scientists to think about applying two different SN curves, one associated to the surface flaws and one to the volume flaws. Such a change of the destructive mechanism may require the mapping of two distributions that describe the micro-damage accumulation.

However, regarding the mapping of the test results, the author believes: A *physical average curve* is the result of a probabilistically-driven strength problem, and is smooth because it is not like a sudden instability problem. Therefore, the course of the cyclic failure test data cannot show some sudden downward ‘jump’. Hence, the continuous four parameter Weibull mapping approach of the SN test data can capture the course

$$R = \text{constant} : \quad \sigma_{\max}(R, N) = c1 + (c2 - c1) / \exp(\log N / c3)^{c4}.$$

Fatigue curves are given for un-notched test specimens ( $K_t = 1$ , like the later examples) and for notched ones. The loading can be uniaxial and can be complex multi-axial stress states.

A suitable ‘permitted’ stress criterion is to apply.

## 2.2 *Relation of the Material Stressing Effort Eff with the Micro-damage D*

There are practically two possibilities to present SN curves: Using in the case of ductile materials (1) the stress amplitude  $\sigma_a(R, N)$ , also termed alternating stress, and in the case of brittle materials (2) the maximum or upper stress  $\sigma_{\max}(R, N)$ , usually termed *fatigue strength*. The maximum stress is physically simpler to understand by the ‘stress man’ than the amplitude, according to smooth transfer from the static to the cyclic behavior, Fig.2. Namely, a decaying SN curve is interpretable like a decaying ‘static’ strength after a micro-damage process with  $n$  cycles.

Thereby, the static material stressing effort *Eff* (Werkstoffanstrengung,  $N_f = 1$ ) is replaced by the accumulated cyclic micro-damage sum  $D(N)$ . Applied here is the classical 4-parameter Weibull curve with one parameter still fixed as strength point origin, because for brittle materials the strength value  $\bar{R}^t = \sigma_{\max}$  ( $n = N = 1$ ) is preferably used as origin in the tension domain and anchor point of the SN curve and in the compression domain  $-\bar{R}^c = \sigma_{\min}$  ( $n = N = 1$ ). In detail, Fig.2 visualizes the transfer from the static load-driven increase of the material stressing effort ( $n = N = 1$ )  $Eff = 100\%$  (expectance value 50%) at the strength point to the cycle-driven micro-damage sum  $D_{\text{mapping}} = 100\%$  (expectance value 50%) of the SN curve. The evolution of *Eff* is not linked to the accumulation of the micro-damage. At onset-of-micro-cracking *Eff* is still  $> 0$ .

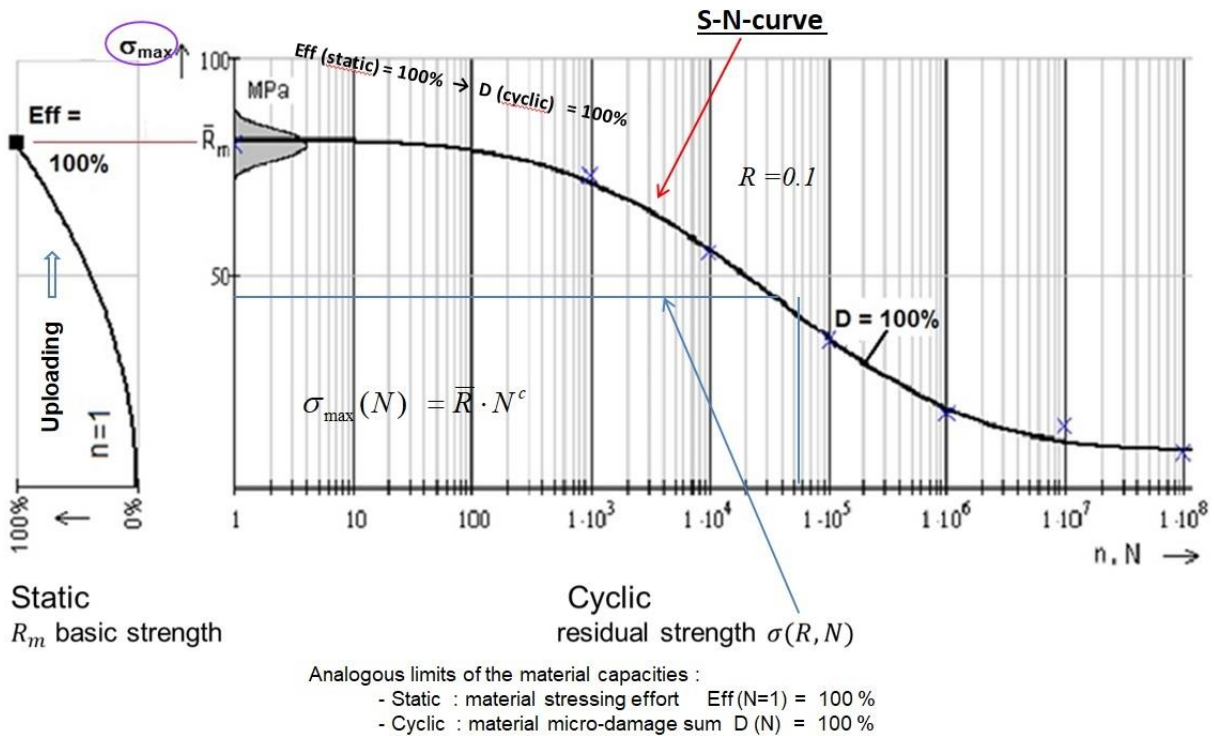


Fig.2, Mapping: Eff versus  $D \equiv D_{\text{mapping}}$ , mapping deals with averages, 50% expectance value

### 2.3 Statistical properties in Design Verification (DV)

As the average SN curve cannot be applied in fatigue life DV, a statistically reduced curve is to determine as design curve, see Fig.3. This design curve is seen as a  $D_{\text{design}} = 100\%$  -SN-curve.

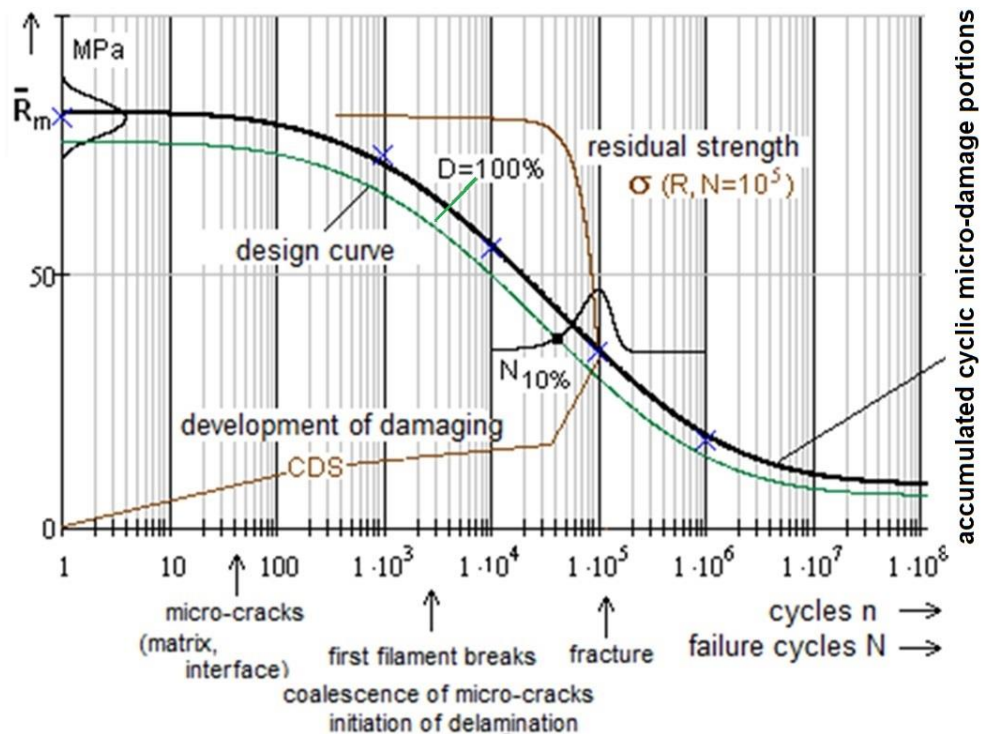


Fig.3, Design Verification: Fatigue average curve and design curve.  $D = D_{\text{design}}$  for a survival probability  $P$  with a confidence level  $C$ . CDS is 'characteristic damage state' of a lamina

Conclusion: It is essential to discriminate mapping and designing.

$$\begin{aligned} \text{Static failure} &\rightarrow \max \sigma = \bar{R}_{\text{sta}}, \text{Eff}_{\text{mapping}} = 1 \text{ (50\%, 50\%)} \Rightarrow \text{cyclic failure} \rightarrow \max \sigma = \bar{R}_{\text{cyc}}, D_{\text{mapping}} = 1 \\ \text{Static failure} &\rightarrow \max \sigma = R_{\text{sta}}, \text{Eff}_{\text{design}} = 1 \text{ (P, C)} \Rightarrow \text{cyclic failure} \rightarrow \max \sigma = R_{\text{cyc}}, D_{\text{design}} = 1. \end{aligned}$$

In design verification DV very often as fractiles (quantiles), to meet a distinct survival failure probability P, values of 5% or 10% are taken in order to capture some uncertainty on the resistance side compared to the average of 50%. For the action (loading) side the design FoS  $j$  capture the uncertainty of the loading.

Capturing the uncertainty of the resistance quantities, the following is performed: Denoting P the survival probability and C the confidence level applied, when estimating a basic population value from several test samples, partly enriched by some knowledge of the basic population and regarding C a one-sided tolerance level it reads:

- \* Static  $\rightarrow$  Statistical reduction of average strength from (P = 50%, C= 50%) to e.g. (P = 90%, C = **95%**).
- \* Cyclic  $\rightarrow$  Statistical reduction of average SN curve from (P =50%, C= 50%) to e.g. (P = 90%, C= **50%**). In order to improve this situation the maximum accumulated micro-damage is firstly reduced in DV from the fictitious theoretical ‘Miner value’  $D = 1 = N_{50} / N_{50}$  (P = 50%, C= 50% with N based on the average curve) to a feasible value  $D_{\text{feasible}}$  (P = 90%, C= **50%**) and further imposed by a FoS  $j_{\text{Life}} > 5$ . This feasible D, linked to the lower design SN curve, is determined by (P = 90%, C = 50%  $\rightarrow D_{\text{feasible}} = N_{90} / N_{50}$  for a distinct  $N_{50}$  value and an associated stress.

### Some Lessons Learned:

- *The Palmgren-Miner rule cannot account for loading sequence effects, residual stresses, and for stresses below the fatigue limit (life  $\rightarrow \infty$  ?)*
- *Whether a material has an endurance fatigue limit is usually open regarding the lack of VHCF tests. As an apparent fatigue strength (scheinbare Dauerfestigkeit) the strength at  $2 \cdot 10^6$  cycles might be only called. However, e.g. CFRP could possess a high fatigue limit.*
- *Designing light-weight structures means a reduction of dead mass. Therefore, the ratio ‘variable load / dead load’ reduces, fatigue becomes more decisive and fatigue life prediction procedures become also more mandatory in construction industry, for instance!*
- *In the LCF regime non-linearity causing effects such as creeping, relaxation are to consider.*
- *Whether the material’s micro-damage driver remains the same from LCF until VHCF must be verified in each given design case.*

### 3 Failure-Mode-Concept (FMC) and static Strength Failure Criteria (SFC)

#### 3.1 Features of the Failure-Mode-Concept

For a better common understanding at first some terms shall be added here: Failure condition: Condition on which a failure becomes effective, meaning  $F = 1$  or  $Eff = 100\%$  for one distinct limit state. Layer: Physical element from winding, tape-laying process, other depositing procedures. Lamina: Designation of the single UD ply as computational element of the laminate, used as laminate subset or building block for modeling and it might capture several equal plies. First-Ply-Failure FPF: First Inter-Fiber-Failure IFF in a lamina of the laminate (*Tsai [10] did not exclude FF*). Simulation: Process, that consists of several analysis loops and lasts until the system behavior is imitated in the Design Dimensioning process. The model parameters are adjusted hereby to the ‘real world’ parameter set. Analysis: Computation that uses fixed model parameters, such as the analysis of the final design.

Modeling of the Variety of Laminates is a challenge. In this context essential for the interpretation of the failures – faced after testing – is the knowledge about the lay-up of the envisaged laminate, crimped and no-crimped materials behave differently. It is further extremely necessary to provide the material-modeling design engineer and his colleague in production (*for his Ply Book*) with a clear, distinguishing description of UD-lay-ups, of NonCrimpFabrics NCFs (*stitched multi-UD-layer*) and of Fabric layers (*crimped*). Due to unclear descriptions the author could often not use valuable test results. As former editor of the VDI guideline 2014 the author makes the following proposal:

- \*Single UD-layers-deposited stack  $[0/90]$ ,  $[0/90]_S = [0/90/90/0]$  lay-up  
(a wavy bracket for each building block ‘deposited UD-layer’ is not necessary)
- \*Semi-finished product, stitched NCF:  $\{0/90\} + \{90/0\}$  symmetrically stacked  
*novel deliverable ‘building blocks’*  $\{0/45/-45/90\}, \{\phi/-\psi/-\phi/\psi\}, \{0/60/-60\}$ , etc  
two stacked NCFs, „Bi – Ax“  $[\{75/-75\}/\{-15/15\}]_r$   
one NCF, r = repetition  $[\{75/-75/-15/15\}]_r$
- \*Semi-finished product, woven Fabric:  $\begin{bmatrix} 0 \\ 90 \end{bmatrix}$ ,  $\begin{bmatrix} 0 \\ 90 \end{bmatrix}_S = \begin{bmatrix} 0 \\ 90 \end{bmatrix}_2, \begin{bmatrix} 45 \\ -45 \end{bmatrix}$   
 $\Rightarrow$  Combination:  $[\begin{bmatrix} 45 \\ -45 \end{bmatrix}]/\{75/-75/-15/15\}]_3/[0/90/90/0]/[\begin{bmatrix} 0 \\ 90 \end{bmatrix}]_2$  .

In the development of structural parts the application of 3D-validated SFCs is one essential pre-condition for achieving the required reliable DV. This includes a Yield Failure Condition (*ductile behavior*) for non-linear analysis of the material and also for design verification at the

limit state ‘Onset-of-Yielding’. It further includes conditions to verify that ‘Onset-of-Fracture’ is not met in the case of brittle and of ductile behavior.

Under the design-simplifying presumption “Homogeneity is a permitted assessment for the material concerned”, and regarding the respective material tensors, it follows from material symmetry that the number of strengths equals the number of elasticity properties!

Fracture morphology gives further evidence: “Each strength property corresponds to a distinct strength failure mode and to a distinct strength failure type, to Normal Fracture (NF) or to Shear Fracture (SF). This means, a characteristic number of quantities is fixed: 2 for isotropic material and 5 for the transversely-isotropic UD lamina ( $\equiv$  lamellas in civil engineering).”

In the case of ideally homogeneous materials a ‘generic’ number seems to be faced. Hence, the applicability of material symmetry involves that in general just a minimum number of properties needs to be measured (*cost + time benefits*), which is helpful when setting up strength test programs. Of course, this is also beneficial regarding material modeling.

The basic features of the FMC, derived about 1995 [1, 2, 11] are:

- Each failure mode represents 1 independent failure mechanism and thereby represents 1 piece of the complete failure surface.
- A failure mechanism at the micro-scopic mode level shall be considered in the applied desired macro-scopic SFC
- Each failure mechanism or mode is governed by 1 basic strength  $R$ , only, and witnessed!
- Each failure mode can be represented by 1 SFC

Therefore, equivalent stresses can be computed for each mode. This is of advantage when deriving SN curves and generating Haigh diagrams in fatigue with minimum test effort in order to relatively effortless obtain Constant Fatigue Life curves, see [1] for lifetime estimation. Modal SFCs lead to a *clear* mode strength-associated equivalent stress

- Of course, a modal FMC-approach requires an interaction in all the mode transition zones or mixed failure domains, respectively, reading

$$Eff = \sqrt[m]{(Eff^{\text{mode } 1})^m + (Eff^{\text{mode } 2})^m + \dots} = 1 = 100\% \quad \text{for Onset-of-Failure .}$$

It employs the so-called ‘material stressing effort’ (*artificial term, generated in the WWFE in order to get an English term for the excellent, meaningful German term Werkstoffanstrengung*).

Analogous to ‘Mises’, follows

$$Eff^{\text{yield mode}} = \sigma_{eq}^{\text{Mises}} / R_{0.2} \quad \rightarrow \quad Eff^{\text{fracture mode}} = \sigma_{eq}^{\text{fracture mode}} / R ,$$

with a mode interaction exponent  $m$ , also termed rounding-off exponent, the size of which is high in case of low scatter and vice versa. The value of  $m$  is obtained by curve fitting of test data in the transition zone of the interacting modes. General FRP mapping experience delivered that  $2.5 < m < 3$ . A lower value chosen for the interaction exponent is more on

the safe Reserve Factor  $RF$  side or more ‘design verification conservative’. For CFRP,  $m = 2.6$  is recommended from mapping experience.

From engineering reasons  $m$  is chosen the same in all transition zones of adjacent mode domains. Using the interaction equation is leading again to a pseudo-global failure curve or surface. In other words, a ‘single surface failure description’ is achieved again, such as with Tsai/Wu but without the shortcomings of this global SFC.

Above interaction of adjacent failure modes is modelled by the ‘series failure system’. That permits to formulate the total material stressing effort  $Eff$  generated by all activated failure modes as ‘accumulation’ of  $Eff = \sum Eff^{modes} \equiv$  sum of the single mode failure danger proportions.  $Eff = 100\% = 1$  represents the mathematical description of the complete surface of the failure body [1, 3]. In practice, i.e. in thin UD laminas, at maximum, 3 modes of the 5 modes ( $2 FF + 3 IFF$ ) will physically interact. Considering 3D-loaded thick laminas embedded in laminates, there, all 3 IFF modes might interact.

### 3.2 Modal and Global SFCs

The HMH yield failure condition can be termed a modal SFC. It captures just one failure mode. The author choose the term “Global“ as a ‘play on words’ to “modal” and to being word-self-explaining. Present SFCs can be basically separated into above two groups, the global (*the German ZTL-SFC in the HSB also belongs to it*) and the modal SFC ones. [1, 11].

All modes are married in the Global formulation.  
Any change hits all mode domains NF and SF of the fracture body surface

Drucker-Prager, Ottosen, Willam-Warnke, Tsai-Wu,  
Altenbach/Bolchun/ Kulupaev, Yu , etc.

1 Global SFC :	$F(\{\sigma\}, \{R\}) = 1$	global formulation, usually
Set of Modal SFCs :	$F(\{\sigma\}, \{R^{mode}\}) = 1$	model formulation in the FMC

Mises,Puck,Cuntze

All modes are separately formulated.  
Any change hits only the relevant domain of the fracture body surface

$$F(\{\sigma\}, \{R^{mode}, \mu^{mode}\}) = 1 \quad \text{more precise formulation}$$

by direct introduction of the friction value  
considering Mohr-Coulomb for brittle materials under compression

$$UD : \quad \{\sigma\} = (\sigma_1, \sigma_2, \sigma_3, \tau_{23}, \tau_{31}, \tau_{21})^T, \quad \{\bar{R}\} = (\bar{R}_{||}^t, \bar{R}_{||}^c, \bar{R}_{\perp}^t, \bar{R}_{\perp}^c, \bar{R}_{\perp||})^T; \mu_{\perp||}, \mu_{\perp\perp})^T$$

$$Isotrop : \{\sigma\} = (\sigma_x, \sigma_y, \sigma_z, \tau_{yz}, \tau_{zx}, \tau_{xy})^T = (\sigma_I, \sigma_{II}, \sigma_{III})^T, \quad \{\bar{R}\} = (\bar{R}^t, \bar{R}^c; \mu)^T$$

Needs an interaction of Failure Modes:

This is performed by a probabilistic approach (series failure system) in the transition zones between neighboring modes NF and SF

*Fig.4: ‘Global’ and ‘Modal’ SFCs*

*Fig.4* presents the main differences between these SFC types. Global SFCs describe the full failure surface by one single mathematical equation. This means that for instance a change of the UD *tensile* strength  $\bar{R}'_{\perp}$  affects the failure curve in the *compression* domain, where no physical impact can be! In this context, the computed *RF* may not be on the safe side in this domain. This shortcoming of the global SFCs caused the author to create modal ones.

Often, SFCs employ just strengths and no friction value. This is physically not accurate. Mohr-Coulomb acts in the case of compressed brittle materials! The undesired consequence in Design Verification again is: The computed *RF* may be not on the safe side.

### 3.3 FMC-based Failure Modes, SFCs and SFC-visualization

#### 3.3.1 Types of Failure Modes

Since two decades the author believes in a macroscopically-phenomenological ‘complete classification’ system, where all strength failure types are included, see *Fig.5*. In his assumed system several relationships may be recognized: (1) shear stress yielding SY, followed by shear fracture SF viewing ‘dense’ materials. For porous materials under compression, the SF for dense materials is replaced by crushing fracture CrF. (2) However, to complete a system beside SY also NY should exist. This could be demonstrated by the author for PMMA (plexiglass) with its chain-based texture showing NY due to crazing failure [1].

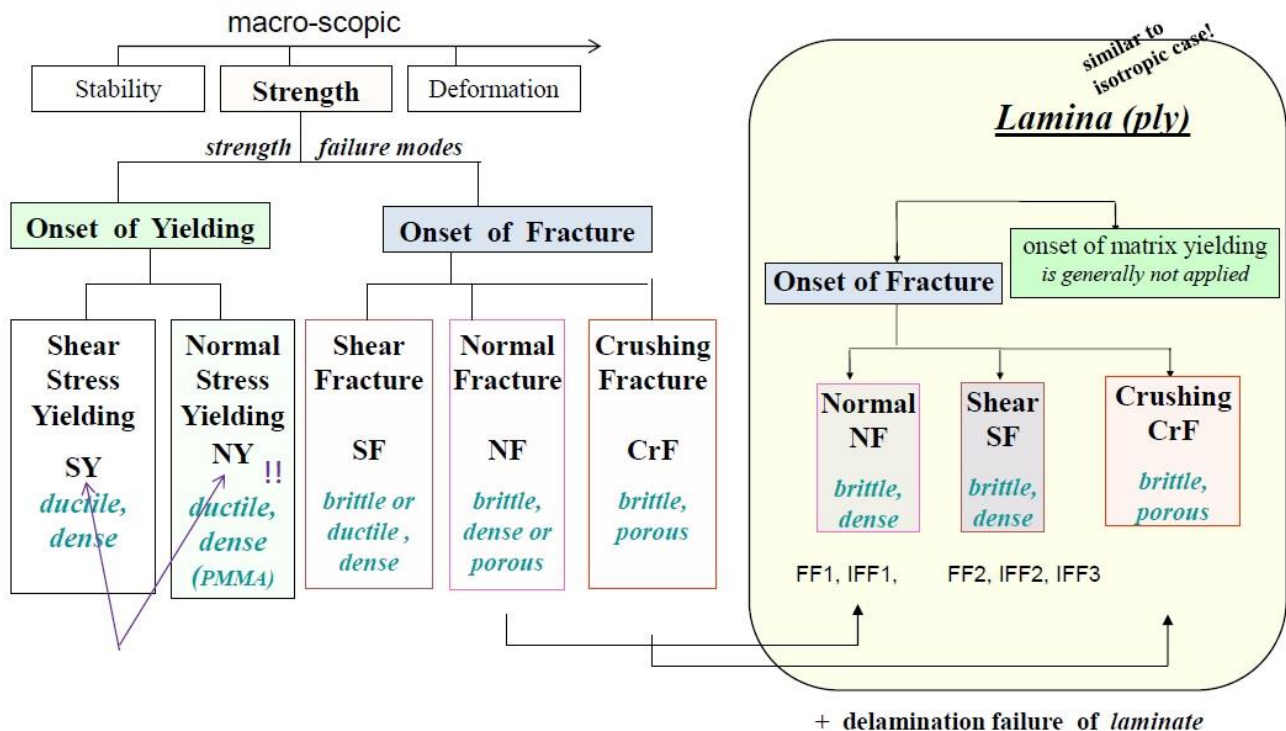


*Fig.5: Proposed scheme of macro-scopic strength failure modes of isotropic materials and transversely-isotropic UD-materials (Cuntze1998)*

The right side of the scheme shows that a full similarity of the ‘simpler’ isotropic materials with transversely-isotropic UD materials exists. The strength failure modes involve a similar variety of fracture strength failure types such as SY, NF.

Of interest is not only the interaction of the fracture surface portions in a *mixed* failure domain or transition zone of adjacent failure modes, respectively, but failure in a *multi-fold* failure domain (superscript <sup>MFFD</sup>) such as at  $\sigma_1 = \sigma_{II}$ . There the associated mode material stressing effort acts twofold. It activates failure in two orthogonal directions which is to consider by adding a multi-fold failure term in each of the present SFCs, proposed in [11, 12] for isotropic materials. It can be applied as well to brittle UD-material in the quasi-isotropic transversal plane  $\sigma_2 = \sigma_3$ .

### 3.3.2 FMC-based SFCs and their Visualization

First and usual assumption for the material models is an ideally homogeneous solid. Following Beltrami and Mohr-Coulomb the solid material element may experience, generated from different energy portions, a shape change, a volume change and friction and these can be linked to invariants, which is of great advantage [1, 13].

For the here basically envisaged UD material the applied invariants from Boehler read:  $\sigma_2 = \sigma_{\perp}$

$$I_1 = \sigma_1, I_2 = \sigma_2 + \sigma_3, I_3 = \tau_{31}^2 + \tau_{21}^2, I_4 = (\sigma_2 - \sigma_3)^2 + 4 \cdot \tau_{23}^2, I_5 = (\sigma_2 - \sigma_3) \cdot (\tau_{31}^2 - \tau_{21}^2) - 4\tau_{23}\tau_{31}\tau_{21}$$

Table 1 collects the FMC-derived 5 UD-SFC formulations.

*Table 1 ‘Dense’ UD materials: SFC formulations for FF1, FF2 and IFF1, IFF2, IFF3*

$$\text{FF1: } Eff^{\parallel\sigma} = \check{\sigma}_1 / \bar{R}_{\parallel}^t = \sigma_{eq}^{\parallel\sigma} / \bar{R}_{\parallel}^t \quad \text{with} \quad \check{\sigma}_1 \cong \varepsilon_1^t \cdot E_{\parallel} \quad (\text{matrix neglected})$$

$$\text{FF2: } Eff^{\parallel\tau} = -\check{\sigma}_1 / \bar{R}_{\parallel}^c = +\sigma_{eq}^{\parallel\tau} / \bar{R}_{\parallel}^c \quad \text{with} \quad \check{\sigma}_1 \cong \varepsilon_1^c \cdot E_{\parallel} \quad (\text{corresponds to a SF})$$

$$\text{IFF1: } Eff^{\perp\sigma} = [(\sigma_2 + \sigma_3) + \sqrt{\sigma_2^2 - 2\sigma_2 \cdot \sigma_3 + \sigma_3^2 + 4\tau_{23}^2}] / 2\bar{R}_{\perp}^t = \sigma_{eq}^{\perp\sigma} / \bar{R}_{\perp}^t$$

$$\text{IFF2: } Eff^{\perp\tau} = [a_{\perp\perp} \cdot (\sigma_2 + \sigma_3) + b_{\perp\perp} \sqrt{\sigma_2^2 - 2\sigma_2 \sigma_3 + \sigma_3^2 + 4\tau_{23}^2}] / \bar{R}_{\perp}^c = \sigma_{eq}^{\perp\tau} / \bar{R}_{\perp}^c$$

$$\text{IFF3: } Eff^{\perp\parallel} = \{ [b_{\perp\parallel} \cdot I_{23-5} + (\sqrt{b_{\perp\parallel}^2 \cdot I_{23-5}^2 + 4 \cdot \bar{R}_{\perp\parallel}^2 \cdot (\tau_{31}^2 + \tau_{21}^2)^2}) / (2 \cdot \bar{R}_{\perp\parallel}^3) ] \}^{0.5} = \sigma_{eq}^{\perp\parallel} / \bar{R}_{\perp\parallel}$$

$$\left\{ \sigma_{eq}^{\text{mode}} \right\} = \left( \sigma_{eq}^{\parallel\sigma}, \sigma_{eq}^{\parallel\tau}, \sigma_{eq}^{\perp\sigma}, \sigma_{eq}^{\perp\tau}, \sigma_{eq}^{\perp\parallel} \right)^T, \quad I_{23-5} = 2\sigma_2 \cdot \tau_{21}^2 + 2\sigma_3 \cdot \tau_{31}^2 + 4\tau_{23}\tau_{31}\tau_{21}$$

Inserting the compressive strength point  $(0, -\bar{R}_{\perp}^c) \rightarrow a_{\perp\perp} \cong \mu_{\perp\perp} / (1 - \mu_{\perp\perp})$ ,  $b_{\perp\perp} = a_{\perp\perp} + 1$  from a measured fracture angle  $\rightarrow \mu_{\perp\perp} = \cos(2 \cdot \theta_{fp}^c \cdot \pi / 180)$ , for  $50^\circ \rightarrow \mu = 0.174$ .

$$b_{\perp\parallel} \cong 2 \cdot \mu_{\perp\parallel}. \quad \text{Typical friction value ranges: } 0 < \mu_{\perp\parallel} < 0.25, \quad 0 < \mu_{\perp\perp} < 0.2.$$

‘Porous’ UD material [1, 4]: Replacement of **IFF2** by using

$$Eff_{porosity}^{SF} = \sqrt{a_{\perp\perp por}^2 \cdot I_2^2 + b_{\perp\perp por}^2 \cdot I_4 - a_{\perp\perp por} \cdot I_2} / 2\bar{R}_{\perp}^c.$$



A measurable friction value  $\mu$  tells the engineer much more than a fictitious friction parameters  $b$ . This encouraged the author to transfer the structural stresses-formulated UD-fracture curve  $\sigma_2(\sigma_3)$  into a Mohr-Coulomb one obtaining  $\tau_{nt}(\sigma_n)$ , [1, §??]. This novel, mathematically pretty effortful transformation enabled to link the parameter  $b$  of the respective SFCs via a determined shear fracture angle to the measurable physical friction value  $\mu$ .

Delamination within a laminate may occur in tensile-shear cases and compression-shear cases (*remember the so-called wedge failure IFF2 of Puck with its inclined fracture plane* [7, 14]). Considering such a delamination a 3D stress state is to be regarded. This is especially the case if bends in the structure are stretched or compressed which generates stresses across the wall thickness. These stresses are activated by the delamination-critical inter-laminar stress state

Before using UD-SFCs some pre-requisites are to check to really achieve *reliable* results. This is still valid for the SFC model-validation by the test specimens and for the verification of the laminate designs:

- Good fiber placement and alignment, and uniform distribution
- ‘*Fabrication signatures*’ such as fabrication-induced fiber waviness and wrinkles are small and do not vary in the test specimens
- If applicable, residual stresses from the curing cycle are to be computed for the difference ‘*stress free temperature to room temperature 22°C*’ as an effective temperature difference. Considering curing stresses or moisture stresses, the specimens are most often assumed to be well conditioned
- The stress-strain curves are average curves in design dimensioning, which is also the type one needs for test data mapping in order to obtain the best estimation for the structural response, namely 50%.

Fig.6 depicts the fracture failure body of UD materials. The upper picture contains the failure body of the plane 2D stress state and the lower picture the body of the 3D stress state. These look the same and are the same. One must only replace the UD-lamina stresses of the 2D-case by equivalent stresses to obtain the 3D-**fracture failure body**.

$$\{\sigma\}_{\text{lamina}} = (0, \sigma_2, \sigma_3, \tau_{23}, \tau_{31}, \tau_{21})^T .$$

### 3.3.3 Static Validation of the FMC-based SFCs in the World-Wide-Failure-Exercises (WWFEs)

The author validated his FMC-based SFCs for a large variety of isotropic brittle structural materials such as plexiglass, porous concrete stone, cast iron, Normal Concrete, UHPC sandstone, mild steels, foam, monolithic ceramics and for the transversely-isotropic UD fiber-reinforced polymers Lamina (ply, lamella) and orthotropic ceramic Fabrics. This was possible as far as available multi-axial fracture test data could be obtained, [1, 4].

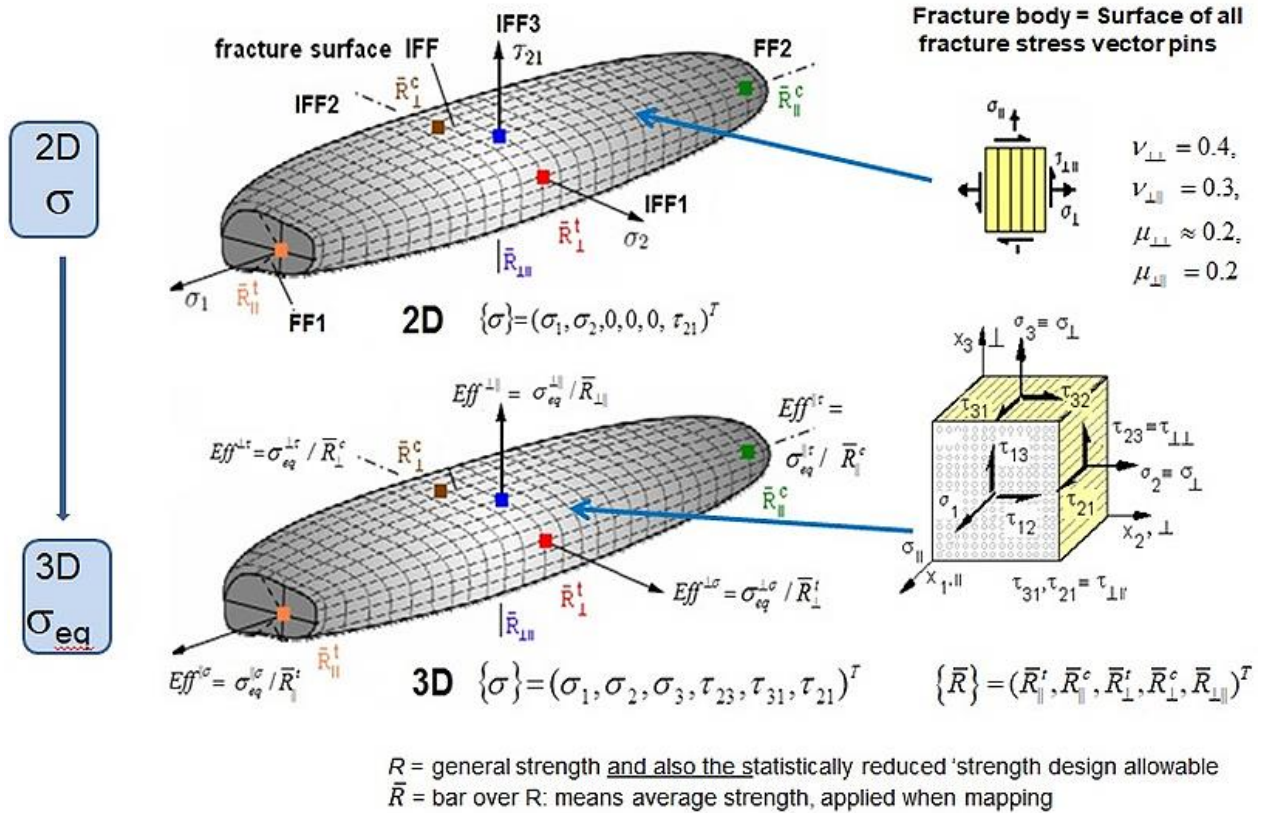


Fig.6: 2D and 3D fracture failure surface (body) and essential UD entities

Basis for the validation of the SFCs for the UD lamina material were own test data and those from the WWFEs. There are three WWFEs that have been executed since 1992: WWFE-I for testing strength fracture criteria by checking the mapping quality of 2D-fracture stress states of the lamina. Then WWFE-II for 3D-fracture stress states for achieving 3D-lamina model validation and some verification by laminate Test Cases. The ongoing WWFE-III is on SFCs generated from Continuum (micro-)Damage Mechanic modelling.

Addressing the WWFE it must be noted again: Model validation = 'qualification' of a generated model by well mapping physical test results with the model. (design) Verification = fulfilment of a set of design requirement data.

And regarding above two WWFEs it is further to note considering the SFC mapping task: \*Part A, a blind prediction had to be made without provision of all needed properties. With the provided strength values alone – in general - a SFC cannot be validated, compression requires a friction information, that was not given. \*Part B, the comparison Theory-Test: Test data sets were partly not applicable or even involved false failure points. More than 50% could not be used without specific care. Further, for instance in WWFE-I TC1 apples and oranges have been put together. One cannot depict in the same diagram 90°-wound tube test specimen data together

with 0°- wound tube data and this happened again with WWFE-II TC2. Due to a careful checking of the provided test data the author achieved the highest number of points in WWFE-I. In the WWFE-II a real assessment of the various SFC-contributions is more or less missing. The author was one of the best contributors.

### 3.4 Application of the Static UD-SFCs to determine Cyclic micro-damage Portions

A very essential question in the estimation of lifetime is a means to assess the micro-damage portions occurring under cycling.

For brittle behavior the response from practice is “It possible to apply validated static SFCs?”

*“If the failure mechanism of a mode cyclically remains the same as in the static case, then the fatigue micro-damage-driving failure parameters are the same and the applicability of static SFCs is allowed for quantifying micro-damage portions”.*

*Thereby it is to note that FMC-based static SFCs apply the equivalent stresses of a mode SF or NF.*

For clarification, the determination of the  $Eff^{mode}$ -values, representative later also for the estimation of micro-damage portions is exemplarily described below for a simple example:

*Table 2: Static Design Verification-procedure with determination of  $Eff^{mode}$ -values*

- Assumption: Linear analysis permitted, design FoS  $j = 1.25$
- \* 2D-stress state:  $\{\sigma\} = (\sigma_1, \sigma_2, \sigma_3, \tau_{23}, \tau_{31}, \tau_{21})^T \cdot j = (0, -60, 0, 0, 0, 50)^T$
- \* Residual stresses: 0 (effect vanishes with increasing micro – cracking)
- \* Strengths:  $\{R\} = (R_{||}^t, R_{||}^c, R_{\perp}^t, R_{\perp}^c, R_{\perp||})^T = (1050, 725, 32, 112, 79)^T$  MPa  
 $\{\bar{R}\} = (1378, 950, 40, 125, 97)^T$  estimated from average values
- \* Friction values :  $\mu_{\perp||} = 0.3, (\mu_{\perp\perp} = 0.35),$  Mode interaction exponent:  $m = 2.7$
- \*  $Eff^{\perp\sigma} = \frac{\sigma_2 - |\sigma_2|^*}{2 \cdot \bar{R}_{\perp}^t} = 0, Eff^{\perp\tau} = \frac{-\sigma_2 + |\sigma_2|}{2 \cdot \bar{R}_{\perp}^c} = 0.60, Eff^{\perp||} = \frac{|\tau_{21}|}{\bar{R}_{\perp||} - \mu_{\perp||} \cdot \sigma_2} = 0.51$
- $Eff^m = (Eff^{\perp\sigma})^m + (Eff^{\perp\tau})^m + (Eff^{\perp||})^m$
- $\Rightarrow Eff = 0.72, RF = 1 / Eff = 1.39, MoS = RF - 1 = 0.39$  (must be positive!).

## 4 FMC-based Constant-Fatigue-Life Estimation Model for UD-ply-composed Laminates

### 4.1 Idea of an Automatic Establishment of Constant Fatigue Life Curves

Basic aim in fatigue design is to reduce the test amount of SN-curves to a minimum. This was a long-lasting task for the author and was firstly solved some years ago. The failure model thinking in the FMC with its derived static SFCs able to assess the micro-damage portions was the first hurdle to tackle.

An analytical, automatic establishment of a continuous Constant Fatigue Life (CFL) curve  $\sigma_a(\sigma_m, N = \text{constant})$  - basis of lifetime estimations - could then be developed ( $N$  is failure cycle number and  $n$  running cycle number). At first a suitable function for mapping the course of provided SN-curve test data was searched. Chosen was the 4-parameter Weibull curve model. A further task in order to reduce the test amount was finding a physically-based model to predict other SN curves, required for fatigue analysis, on basis of probably just one Master SN curve for each mode.

Finally, a challenging task was the very difficult mapping of the *test data decrease* in the so-called transition zone where the modes interact around the stress ratio beam  $R_{\text{transition}} = -R^c / R^t < R = \sigma_{\text{min}} / \sigma_{\text{max}} = -1$ . The traditional investigated beam  $R = -1$  is too more right in the Haigh diagram, see [Fig.9](#), and therefore does not accurately characterize the transition zone in the case of large strength ratio  $R^c / R^t$ . The transition zone is the most problematic modeling region in the Haigh diagram. A solution became possible by a mode decay function which physically terminates the influence of the SF part (*compression*) in the Haigh diagram when the NF part begins to act at  $R = 0$  and vice versa for the NF part (*tension*) at  $R = \infty$ .

In aircraft industry, for a design-necessary interpolation in order to achieve CFL curves, much effort is spent to map them piece-by-piece by straight lines, see for instance the respecting sheets on metals in the HSB (H. Hickethier: *Interpolation and Extrapolation of SN data*). Regarding curved lines, the dissertation of C. Hahne [15] is recommended. Therefore, an automatic possibility to generate realistic continuous CFL-curves is highly desired in order to avoid difficult interpolations between the curves. A reliable procedure would help to save test cost and development time.

For the ‘multiple failure mode suffering’ brittle materials an automatic establishment of the non-piecewise straight CFL curves in Haigh Diagrams is searched – generally applicable to brittle isotropic materials including for instance concrete and UD-materials.

The detailed points of the author for achieving these CFL curves are:

- Measurement of a minimum number of SN curves ( $R = const$ , Einstufenversuch)
- Finding a physically-based model to predict other SN curves, required for fatigue analysis, on basis of a measured ‘Master SN curve’ of each mode. Presumption: An appropriate Master SN curve for each failure mode domain, namely compression (SF) and tension (NF), is available
- Provision of a means how the cycling-caused micro-damage portions can be quantified (see before §3.4)
- Mapping of the test data in the transition domain as *most problematic region in the Haigh diagram*, where the modes interact a practicable mode domain decay function is looked for to regard the opposite decay of the modes
- Final step is the provision of a program that automatically delivers the CFL curves.

#### 4.2 SN curves, derived with Kawai’s Model ‘Modified Fatigue Strength Ratio $\Psi$ ’

Some years ago Misamichi Kawai [16] informed the author on his physically-based model to capture SN-curves. It was dedicated to UD material. His first step was to formulate a ‘Fatigue Strength Ratio’  $\psi$ . This means a normalization of the fatigue strength  $\sigma_{max}(N)$  by a static strength  $\psi = \sigma_{static} / \bar{R} = 1$  ( $\equiv Eff$ ) and such referring to *Eff*. The second step was the formulation of his ‘Modified Fatigue Strength Ratio’  $\Psi$ , which is a reformulation in order to get the stress ratio  $R$  into the static concept  $\psi = (\sigma_a + \sigma_m) / \bar{R} = 1$

$$\Rightarrow 1 = (\sigma_a + \sigma_m) / \bar{R} \Rightarrow \sigma_a / (\bar{R} - \sigma_m) = \Psi \text{ as } \textit{ratio cyclic part} / \textit{'static' part}.$$

For visualization of  $\Psi$  see [Fig.7](#)

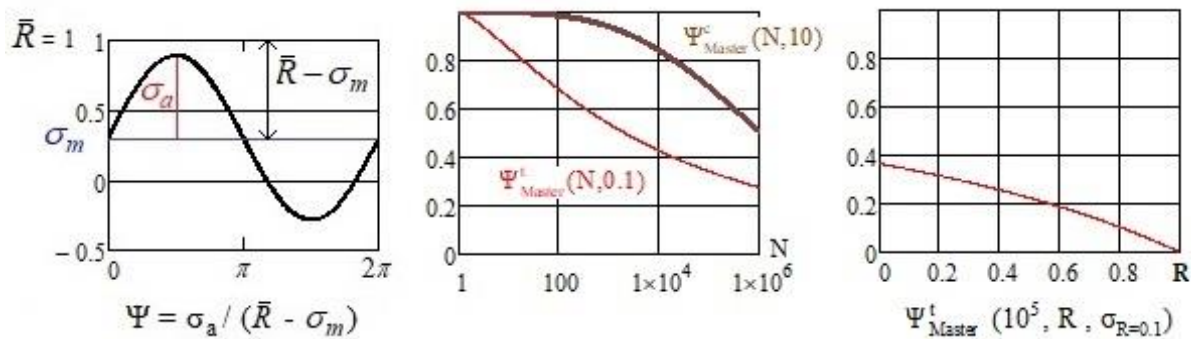


Fig.7: Definition and visualization of ‘Modified Fatigue Strength Ratio  $\Psi$ ’ (ordinate)

Each measured SN-curve is normalized by its static strength  $R$  and the ‘bulk’ of available SN curves then fitted to obtain the Master curve (*hopefully is more than one SN curve measured within the domains and in the transition zone*). Kawai used all  $R$ -curves to obtain  $\Psi = \Psi(R_{fit})$ , independent of the inherent failure mode. Whether it practically makes sense to determine a Master curve by globally fitting all curves is to check, if enough test data will be available considering tension with  $R = 0.1, 0.5$ , compression with  $R=10$  and in the transition zone  $R = -1$

and  $R_{\text{trans}}$ . Due to sticking to the FMC means to stick to a mode domain separation. This requires to tackle the transition zone between the modes separately.

Table 3 presents the determination of SN-curves on basis of  $\Psi$ -model and Master SN-curve.

Table 3: Determination of SN curves on basis of Kawai's  $\Psi$ -model with Master SN curve. Full procedure of the automatic determination of a CFL curve

\* Relationships with stress ratio R

$$\sigma_{\max} = \Delta\sigma / (1 - R) \equiv 2 \cdot \sigma_a / (1 - R) \quad \text{with} \quad \Delta\sigma = \text{stress range, } \sigma_a \text{ is positive}$$

$$R = (\sigma_m - \sigma_a) / (\sigma_m + \sigma_a), \quad \sigma_a = \sigma_m \cdot (1 - R) / (1 + R)$$

$R = -1$ , fully reversed alternating stress.  $R = 0$ ,  $R = 100 (\infty)$ , extreme swelling stresses.

$$\bar{R}^t = \sigma_{\max} (n = N = 1), \quad \bar{R}^c = \sigma_{\min} (n = N = 1)$$

$$\sigma_a = 0.5 \cdot \sigma_{\max} \cdot (1 - R), \quad \sigma_m = 0.5 \cdot \sigma_{\max} \cdot (1 + R); \quad \sigma_a = -0.5 \cdot \sigma_{\min} \cdot (1 - R^{-1}), \quad \sigma_m = \sigma_{\min} (1 - 0.5 \cdot (1 - R^{-1}))$$

\* Choice of problem-adequate mapping function and individual mapping of course of test data

$$\sigma_{\max}(N) = c1 + (\bar{R} - c1) / \exp\left(\frac{\log(N)}{c3}\right), \quad \sigma_{\min}(N) = c1 + (-\bar{R} - c1) / \exp\left(\frac{\log(N)}{c3}\right)^{c2}$$

\* Test input and mapping of available Master curves (usually just available for  $R=0.1$  and  $10$ )

$$\sigma_{R=0.1} = c_1^{NF} + (\bar{R}^t - c_1^{NF}) / \exp\left(\frac{\log(N)}{c_3^{NF}}\right)^{c_2^{NF}}, \quad \sigma_{R=10} = c_1^{SF} + (-\bar{R}^c - c_1^{SF}) / \exp\left(\frac{\log(N)}{c_3^{SF}}\right)^{c_2^{SF}}$$

\* Mode dedicated Application of Kawai's model  $\psi = \sigma / \bar{R}$ ;  $\psi, \Psi$  positive

Static failure occurs at  $\sigma_{\max} = \bar{R}^t = \sigma_a + \sigma_m$  and  $\sigma_{\min} = -\bar{R}^c = -\sigma_a + \sigma_m$ .

$$\sigma_{\max} = \bar{R}^t = \sigma_a + \sigma_m \rightarrow \sigma_a = \bar{R}^t - \sigma_m \rightarrow 1 = \sigma_a / (\bar{R}^t - \sigma_m) \equiv \text{cyclic / 'static'}$$

Kawai's cyclic danger intensity to fail ( $N > 1$ ) is given for tension and compression

$$\Psi_{\text{Master}}^t = \sigma_a / (\bar{R}^t - \sigma_m) \quad \text{and} \quad \Psi_{\text{Master}}^c = \sigma_a / (\bar{R}^t + \sigma_m).$$

\* Relationship of available Master curves with  $\Psi$

Inserting  $\sigma_a, \sigma_m$  brings the stress ratio R into the model

$$\Psi_{\text{Master}}^t = 0.5 \cdot \sigma_{\max}^{\text{Master}} \cdot (1 - R) / [\bar{R}^t - 0.5 \cdot \sigma_{\max}^{\text{Master}} (1 + R)]$$

$$\Psi_{\text{Master}}^c = \sigma_{\min}^{\text{Master}} \cdot (1 - R) / [2 \cdot R \cdot \bar{R}^c + \sigma_{\min}^{\text{Master}} \cdot (1 + R)].$$

\* Resolution of above equations for a novel S-N curve or of a CFL curve (inserting  $\sigma_a, \sigma_m$ )

$$\sigma_{\text{NFdomain}} = 2 \cdot \bar{R}^t \cdot \Psi_{\text{Master}}^t / (\Psi_{\text{Master}}^t - R + R \cdot \Psi_{\text{Master}}^t + 1), \quad 0 < R < 1$$

$$\sigma_{\text{SFdomain}} = -2 \cdot \bar{R}^c \cdot R \cdot \Psi_{\text{Master}}^c / (\Psi_{\text{Master}}^c + R + R \cdot \Psi_{\text{Master}}^c - 1)$$

$$\sigma_{R=0} = 2 \cdot \bar{R}^t \cdot \Psi_{\text{Master}}^t / (\Psi_{\text{Master}}^t - 0 + 0 \cdot \Psi_{\text{Master}}^t + 1) \quad \text{for } R = 0$$

$$\sigma_{R=100} = -2 \cdot \bar{R}^c \cdot 100 \cdot \Psi_{\text{Master}}^c / (\Psi_{\text{Master}}^c + 100 + 100 \cdot \Psi_{\text{Master}}^c - 1) \quad \text{for } R = 100 (\approx \infty).$$

To justify the general applicability of the Kawai model-predicted SN curves, here the 'FMC mode-dedicated' ones, the curves in Fig.8 have been numerically derived. Fig.8 shows the

Master SN curves and the predicted SN curves. With respect to the authors mode dedication the transition beam  $R = -1$  is consequently not depicted in the figure.

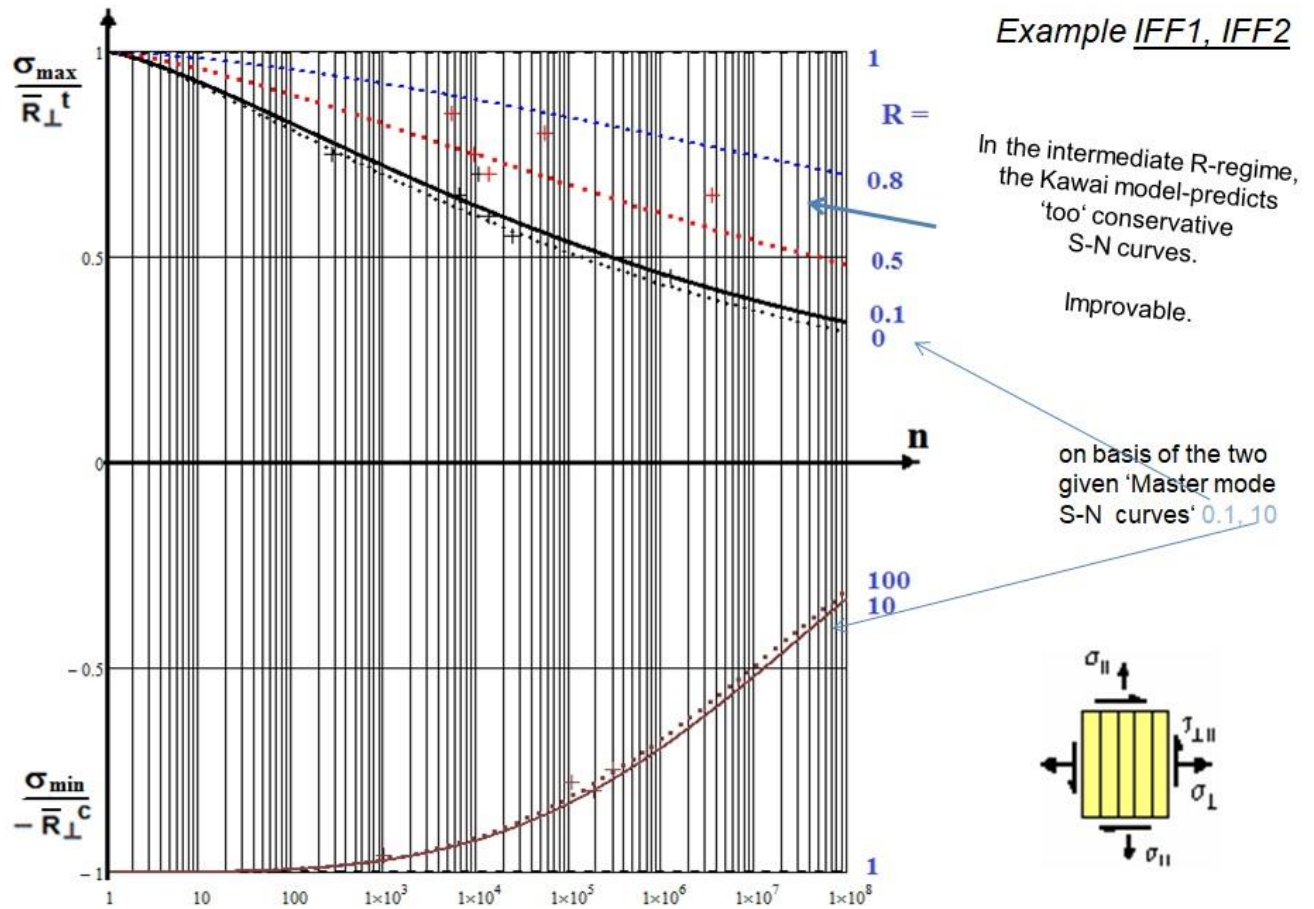


Fig.8: Mode-dedicated Kawai model-derived SN curves. + R=0.5 test data, +R=0.1 test data.

The application results for IFF mode domains demonstrate:

- Limit Curves  $R = 1, 0$  and  $100 (\infty), 1$  are automatically captured
- The question, whether the intermediate Kawai-curves in the range between the limit curves and  $R = 1$  are good enough, can be only responded by further test results and associated modeling research work
- The question, whether Kawai's global fit of all available SN curves is satisfactory could be not supported due to lack of test data. Kawai's model would make it possible to also predict the SN curves in the transition zone  $\infty > R > 0$ .

→ Kawai's model quality looks very promising.

Mind, please: Testing conventionally requires 5 different stress amplitude levels for a distinct SN curve with three repetitions at each level considered as the minimum.

To become practical an IFF work case of a fatigue life estimation shall be presented. It represents the Design Verification of a critically cycled UD lamina embedded within a chosen laminate:

Table 4: Lifetime Design Verification-procedure for a tensioned UD lamina

IFF1: Test data, courtesy C. Hahne

- \* Given:  $\sigma_2 = \sigma_{2a} + \sigma_{2m}$ ,  $\bar{R}_\perp^t = 51$  MPa  
 $n_1 = 50000$  cycles,  $R = 0.5$ ,  $\sigma_2 = 32$  MPa;  $n_2 = 100000$  cycles,  $R = 0$ ,  $\sigma_2 = 30$  MPa

$$\sigma_{\max}^{\text{Master}} = c1 + (\bar{R}_\perp^t - c1) / \exp\left(\frac{\log(N)}{c3}\right)^{c2} \quad \text{with } c1 = 7.1, c2 = 1.34, c3 = 6.05$$

$$\Psi_{\text{Master}}^t = \frac{\sigma_{2a}}{\bar{R}_\perp^t - \sigma_{2m}} = 0.5 \cdot \sigma_{\max}^{\text{Master}} \cdot (1 - R) / (\bar{R}_\perp^t - 0.5 \cdot \sigma_{\max}^{\text{Master}} (1 + R))$$

and after resolution an equation for the determination of a desired S-N curve, inserting R

$$\sigma_{\max} = 2 \cdot \bar{R}_\perp^t \cdot \Psi_{\text{Master}}^t / (\Psi_{\text{Master}}^t - R + R \cdot \Psi_{\text{Master}}^t + 1), \quad 0 < R < 1$$

- \* Estimation of fracture cycles N at  $D_i = n_i / N_i = 100\%$

$$\sigma_{R=0.5} = 2 \cdot \bar{R}_\perp^t \cdot \Psi_{\text{Master}}^t / (\Psi_{\text{Master}}^t - 0.5 + 0.5 \cdot \Psi_{\text{Master}}^t + 1) = \sigma_2 \rightarrow N_1 = 4.6 \cdot 10^5$$

$$\sigma_{R=0} = 2 \cdot \bar{R}_\perp^t \cdot \Psi_{\text{Master}}^t / (\Psi_{\text{Master}}^t - 0 + 0 \cdot \Psi_{\text{Master}}^t + 1) = \sigma_2 \rightarrow N_2 = 1.7 \cdot 10^6$$

- \* Summing up the micro-damage portions  $\rightarrow \text{total } D_i = \sum n_i / N_i = 0.17 < 1 = 100\%$
- \* From experience with the SN-scatter  $\rightarrow \text{RF}_{\text{Life}}$  should be  $> 5$  (termed 'Relative Miner').

$$\text{DV delivers} \rightarrow \text{RF}_{\text{Life}} = 100\% / \text{total } D = 1 / 0.17 = 6 > 5 !$$

### 4.3 Derivation of Constant Fatigue Life CFL curves in the Transition Domain

There is no problem to establish Haigh diagrams for FF and IFF3 due to the fact 'The strength values are of similar size in each case'. The static interaction formula was almost sufficient. However for a Haigh Diagram for really brittle materials, indicated by the beam  $R_{\text{trans}}$  that is very different to  $R = -1$ , a solution procedure has to be looked for. Chosen was a mode-linked exponentially decaying function  $f_d$ , that practically ends where the other pure mode begins to reign.

As the employment of the decay function is too lengthy in the work case above (Table 4) just two SN curves in the pure tension domain were employed.

Table 5 informs about the steps for an example IFF1-IFF2, where mode interaction has to be taken into account.

In Table 6 the determination of the curve parameters of the mode decay function are derived in the SF and the NF domain and then visualized. In the included figure the resulting curves are displayed.



Table 5: Mode decay function  $f_d$  for tension and compression domain in the Haigh diagram

$$Eff = [(Eff^{NF})^m + (Eff^{SF})^m]^{m^{-1}} = 100\%$$

formulated in amplitude and mean stresses reads

$$\left( \frac{-(\sigma_{2m} - \sigma_{2a}) + |\sigma_{2m} - \sigma_{2a}|}{2 \cdot \bar{R}_\perp^c \cdot f_d} \right)^m + \left( \frac{\sigma_{2m} + \sigma_{2a} + |\sigma_{2m} + \sigma_{2a}|}{2 \cdot \bar{R}_\perp^t \cdot f_d} \right)^m = 1$$

delivering the CFL curve for  $N = 1$  cycle,  $f_d = 1$ , activating both NF with SF.

To obtain a CFL curve for higher  $N$  and larger ratios such as  $R_{trans} = -\bar{R}^c / \bar{R}^t$  above interaction formula, working in the transition zone, is engineering-like to adjust because the action of a mode ends where the other mode begins. Chosen is an exponential decay function  $f_d$  that decays from the end of the pure SF mode at  $R = \infty$  ( $R=10$  possible) down to zero at the beginning of the pure NF mode at  $R = 0$  ( $R=0.1$  possible) and vice versa

$$\rightarrow f_d = 1 / [1 + \exp(\frac{c_1 + \sigma_m}{c_2})]$$

Table 6: Numerical derivation of the parameters of the decay function  $f_d = 1 / [1 + \exp(\frac{c_1 + \sigma_m}{c_2})]$

Vorgabe  $c1sSF := -20$   $c2sSF := -5$

$$0.998 = \frac{1}{1 + e^{\frac{c1sSF - \sigma m105}{c2sSF}}}$$

$$0.01 = \frac{1}{1 + e^{\frac{c1sSF + \sigma m015}{c2sSF}}}$$

AsSF := Suchen(c1sSF, c2sSF)

$$AsSF = \begin{pmatrix} -40.55 \\ -5.553 \end{pmatrix}$$

$c1sSF := AsSF_0$   $c2sSF := AsSF_1$   
 $c1sSF = -40.55$   $c2sSF = -5.553$

Vorgabe  $c1sNF := -20$   $c2sNF := 5$

$$0.01 = \frac{1}{1 + e^{\frac{c1sNF - \sigma m105}{c2sNF}}}$$

$$0.998 = \frac{1}{1 + e^{\frac{c1sNF + \sigma m015}{c2sNF}}}$$

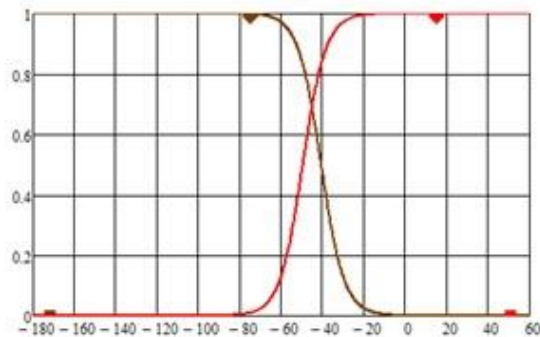
AsNF := Suchen(c1sNF, c2sNF)

$$AsNF = \begin{pmatrix} -49.532 \\ 5.553 \end{pmatrix}$$

$c1sNF := AsNF_0$   $c2sNF := AsNF_1$   
 $c1sNF = -49.532$   $c2sNF = 5.553$

$$fsNFa(\sigma m) := \frac{1}{1 + e^{\frac{c1sNF - \sigma m}{c2sNF}}}$$

$$fsSFa(\sigma m) := \frac{1}{1 + e^{\frac{c1sSF - \sigma m}{c2sSF}}}$$



If static failure  $\rightarrow \max \sigma = \bar{R}_{\text{static}}, \text{Eff} = 1$  and if cyclic failure  $\max \sigma = \bar{R}_{\text{cyclic}}, D = 1$ .

For fully ductile materials no transition zone between 2 modes exists, because just one single mode reigns, namely ‘shear yielding’. There, it is no mean stress effect to correct.

The quality of the approach for the transition zone is practically checked by “How good is the test data course along the stress ratio  $R_{\text{trans}}$ -line mapped?”

Eventually in *Fig.9* mode decay functions  $f_d$  for the tension and the compression domain are displayed. The straight lines in the figure present the extreme SN curve beams,  $R = \infty$  for the SF domain and  $R = 0$  for the NF domain. In between the slightly colored transition zone is located.

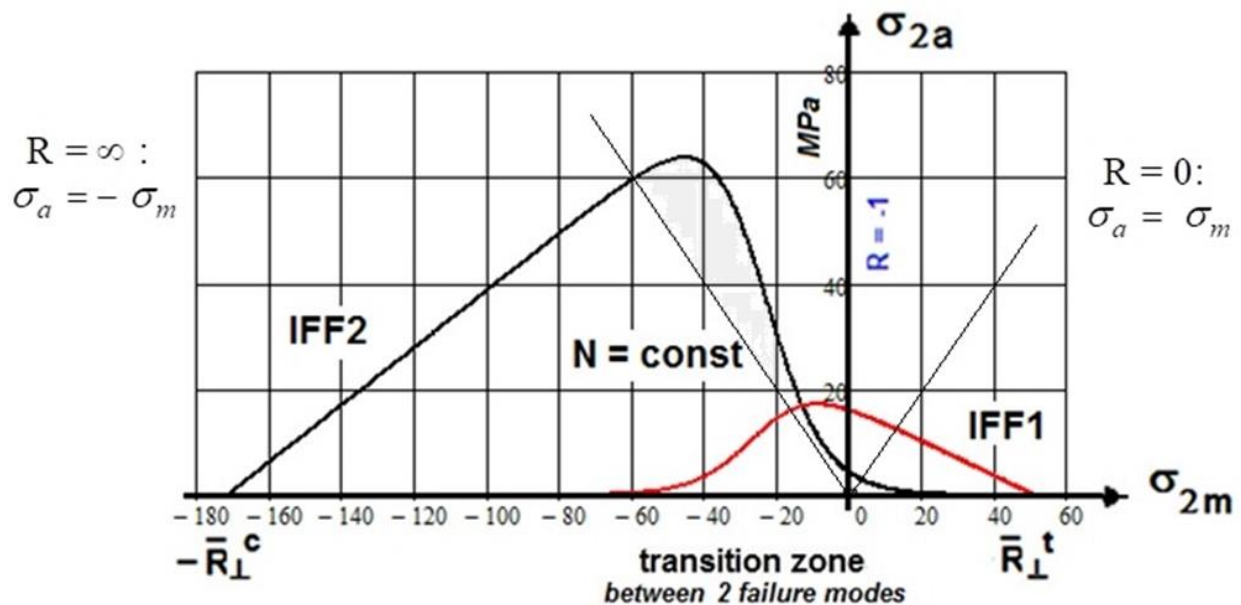


*Fig.9: Effect of the decay function in the transition zone  $-\infty < R < 0$*

The author now proposes his procedure in *Table 7* for deriving part-CFL curve estimates on basis of one Master SN curve provided for each mode. As example a UD-material serves which is stressed in the pure modes IFF1 and IFF2, only.

The transition zone between the modes will be captured in *Table 8*.

Table 7: Estimation of a CFL curve  $\sigma_{2a}$  ( $\sigma_m \equiv \sigma_{2m}$ ,  $N = \text{const}$ ) for IFF,  $N = 10^5$  cycles

- S-N curves in the two Mode Domains IFF1, IFF2

- \* From FMC reasons - in contradiction to Kawai - a strict mode separation is to apply.

- \* S-N curves are generally given for domains IFF1, IFF2 and sometimes  $R = -1$ ,  $R_{\text{trans}}$ . Available Master curves are usually just the standard ones  $R = 0.1$  (IFF1),  $R = 10$  (IFF2)

- \* Computation of the CFL curve parameters for the 2 domains (example  $N = 10^5$ , indexed 5)

$$\sigma_{\max,5}^{\text{Master}}(10^5, R=0.1) = \sigma_{R=0.1}(10^5, R=0.1) = c_1^{\text{NF}} + (\bar{R}^t - c_1^{\text{NF}}) / \exp\left(\frac{\log(10^5)}{c_1^{\text{NF}}}\right)^{c_2^{\text{NF}}} = \bar{R}^t \cdot \Psi_{\text{Master}}^{t,5}$$

$$\sigma_{\min,5}^{\text{Master}}(10^5, R=10) = \sigma_{R=10}(10^5, R=0.1) = c_1^{\text{SF}} + (\bar{R}^c - c_1^{\text{SF}}) / \exp\left(\frac{\log(10^5)}{c_1^{\text{SF}}}\right)^{c_2^{\text{SF}}} = -\bar{R}^c \cdot \Psi_{\text{Master}}^{c,5}$$

- \* The fatigue strengths  $\sigma_{\max}^5(R, 10^5)$ ,  $\sigma_{\min}^5(R, 10^5)$  replace static strengths

$$\sigma_{\max}^5(R) = 2 \cdot \bar{R}^t \cdot \Psi_{\text{Master}}^{t,5} / (\Psi_{\text{Master}}^{t,5} - R + R \cdot \Psi_{\text{Master}}^{t,5} + 1), \quad 0 < R < 1$$

$$\sigma_{\min}^5(R) = -2 \cdot \bar{R}^c \cdot \Psi_{\text{Master}}^{c,5} / (\Psi_{\text{Master}}^{c,5} + R + R \cdot \Psi_{\text{Master}}^{c,5} - 1), \quad 1 < R < 100 (\infty).$$

$$\text{with } R = (\sigma_m - \sigma_{2a,5}) / (\sigma_m + \sigma_{2a,5}).$$

- CFL curves  $\sigma_{\max}^5(R, 10^5)$  within the 2 IFF domains  $\bar{R} \rightarrow \sigma^5(R)$

$$\frac{-(\sigma_{2m} - \sigma_{2a}) + |\sigma_{2m} - \sigma_{2a}|}{2 \cdot \bar{R}_{\perp}^c} = 1 \quad \text{and} \quad \frac{\sigma_{2m} + \sigma_{2a} + |\sigma_{2m} + \sigma_{2a}|}{2 \cdot \bar{R}_{\perp}^t} = 1 \quad \text{static}$$

$$\frac{-(\sigma_{2m} - \sigma_{2a}) + |\sigma_{2m} - \sigma_{2a}|}{2 \cdot \sigma_{\min}^5(R)} = 1 \quad \text{and} \quad \frac{\sigma_{2m} + \sigma_{2a} + |\sigma_{2m} + \sigma_{2a}|}{2 \cdot \sigma_{\max}^5(R)} = 1 \quad \text{cyclic.}$$

- Modelling in the Transition Zone between the mode domains

- \* The transition zone where both the modes interact requires the interaction equation

$$\text{Eff} = [(\text{Eff}^{\text{NF}})^m + (\text{Eff}^{\text{SF}})^m]^{m^{-1}} = 100\% = 1.$$

Formulated in CFL coordinates  $\sigma_a$  and  $\sigma_m$  the static interaction equation reads

$$\left(\frac{-(\sigma_{2m} - \sigma_{2a}) + |\sigma_{2m} - \sigma_{2a}|}{2 \cdot \bar{R}_{\perp}^c}\right)^m + \left(\frac{\sigma_{2m} + \sigma_{2a} + |\sigma_{2m} + \sigma_{2a}|}{2 \cdot \bar{R}_{\perp}^t}\right)^m = 1 \quad \text{static curve, } n = 2N_f.$$

- \* For the  $N = n = 1$  cycle with  $n = 2 \cdot N_f$ : Static interaction equation delivers a curve which still runs through the full Haigh diagram.

- CFL curves in the full Haigh diagram

- \* To obtain a CFL curve for higher  $N$  and larger ratios  $R_{\text{trans}} = -\bar{R}^c / \bar{R}^t$  the two opposite mode decays in the transition zone are to adjust by  $f_d = 1 / [1 + \exp((c_1 + \sigma_m) / c_2)]$ .

- \* Inserting  $R = (\sigma_m - \sigma_{2a,5}) / (\sigma_m + \sigma_{2a,5})$  for  $\sigma_m \rightarrow \sigma_{2m}$  as running variable the CFL curve  $\sigma_{2a}(\sigma_{2m}, N = \text{const})$  is to determine by solving the complicate implicit equation for  $\sigma_{2a}$  below

$$\left(\frac{-(\sigma_{2m} - \sigma_{2a,5}) + |\sigma_{2m} - \sigma_{2a,5}|}{2 \cdot \sigma_{\max}^5(R) / (1 + e^{-\frac{c_{1SF} + \sigma_{2m}}{c_{2SF}}})}\right)^m + \left(\frac{(\sigma_{2m} + \sigma_{2a,5}) + |\sigma_{2m} + \sigma_{2a,5}|}{2 \cdot \sigma_{\max}^5(R) / (1 + e^{-\frac{c_{1NF} + \sigma_{2m}}{c_{2NF}}})}\right)^m = 1.$$

## 5 Complete CFL-curve Model using the Decay Functions $f_d$ in the Haigh-Diagram

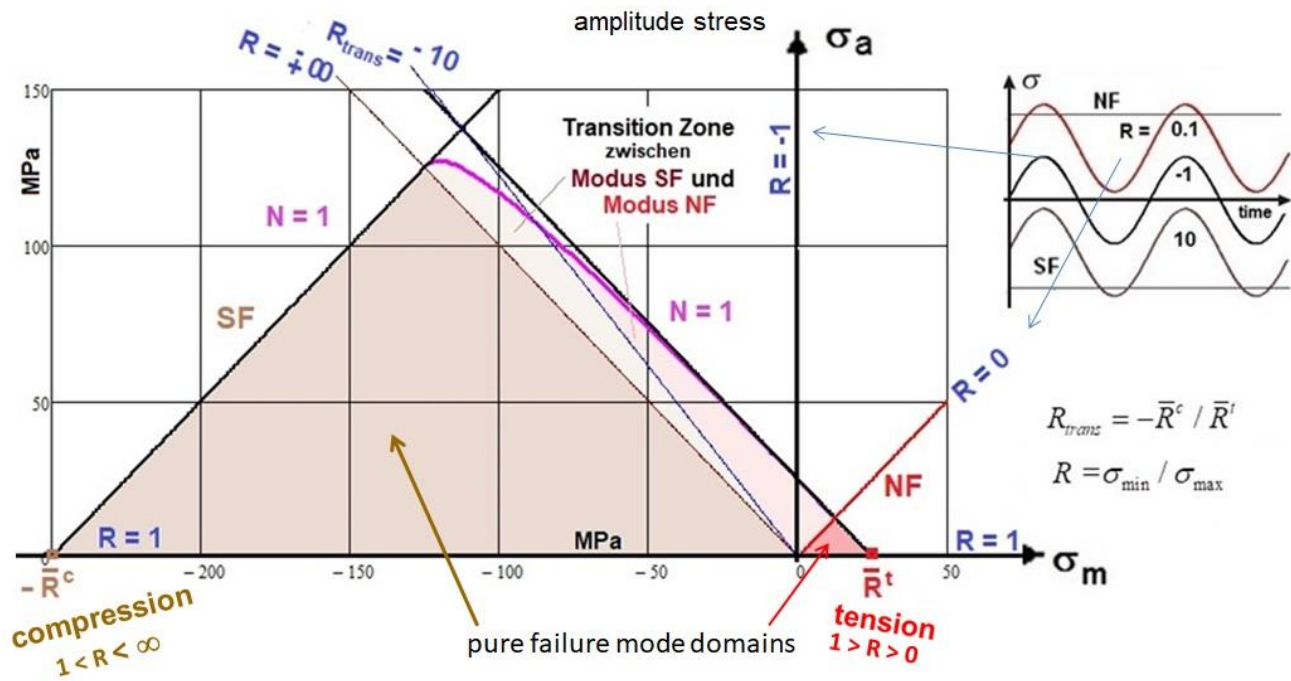
### 5.1 Derivation of the Full Procedure

The Haigh diagram shows the maximum tolerable stress (loading) amplitudes of the material  $\sigma_a(\sigma_m)$ . At first *Fig.10* shall schematically exhibit the pure domains and the transition zone in the Haigh diagram.

For  $N = 1$  the static procedure is applicable using the strength failure envelope represented by the interaction formula. In the negative domain lie the SF-determined SN-curves, in the positive domain the NF determined ones. In the transition zone 2 modes are principally activated which shows either a more SF- or a more NF-determined interaction visualized by the two pale colors. The domain limits are given by the straight SN lines for:

$$R = \infty : \sigma_a = -\sigma_m \quad \text{and} \quad R = 0 : \sigma_a = \sigma_m.$$

The representative SN beams in the transition zone are  $R_{\text{trans}}$  and  $R = -1$ .



**NF = Normal Fracture, SF = Shear Fracture, N = fracture cycle number**

*Fig.10: Scheme for understanding a Haigh-Diagram of a Brittle Isotropic Material  
Up right: alternating stress states of 3 R curves*

Of highest interest are the SN beams in the transition zone around  $R_{\text{trans}}$  and  $R = -1$  which have other origin values than the basic strengths of the modes. The  $R_{\text{trans}}$  origin is not given and has to be determined before mapping. Applied was the static interaction curve,  $N = 1$ , because points on

the boundary must fulfill the static equilibrium. The derivation of the origin points on the side lines reads for the two transition zone beams:

$$R_{\text{trans}} = -\bar{R}_{\perp}^c / \bar{R}_{\perp}^t = -3.4 : \left( \frac{\sigma_{2fr}}{\bar{R}_{\perp}^t} \right)^m + \left( \frac{\sigma_{2fr} \cdot R_{\text{trans}}}{\bar{R}_{\perp}^c} \right)^m = 1 \rightarrow \sigma_{2fr} = -131 \text{ MPa},$$

$$R = -1 : \left( \frac{\sigma_{2fr}}{\bar{R}_{\perp}^t} \right)^m + \left( \frac{\sigma_{2fr} \cdot R}{\bar{R}_{\perp}^c} \right)^m = 1 \rightarrow \sigma_{2fr} = 50.1 \text{ MPa}.$$

In *Fig.11* two CFL-curves are displayed, the envelope  $N = 1$  and  $N = 10^7$ . The pure mode domains are colored and the transition zone is separated by  $R_{\text{trans}}$  into two influence parts. The course of the R-value in the Haigh diagram is represented by the bold dark blue lines.

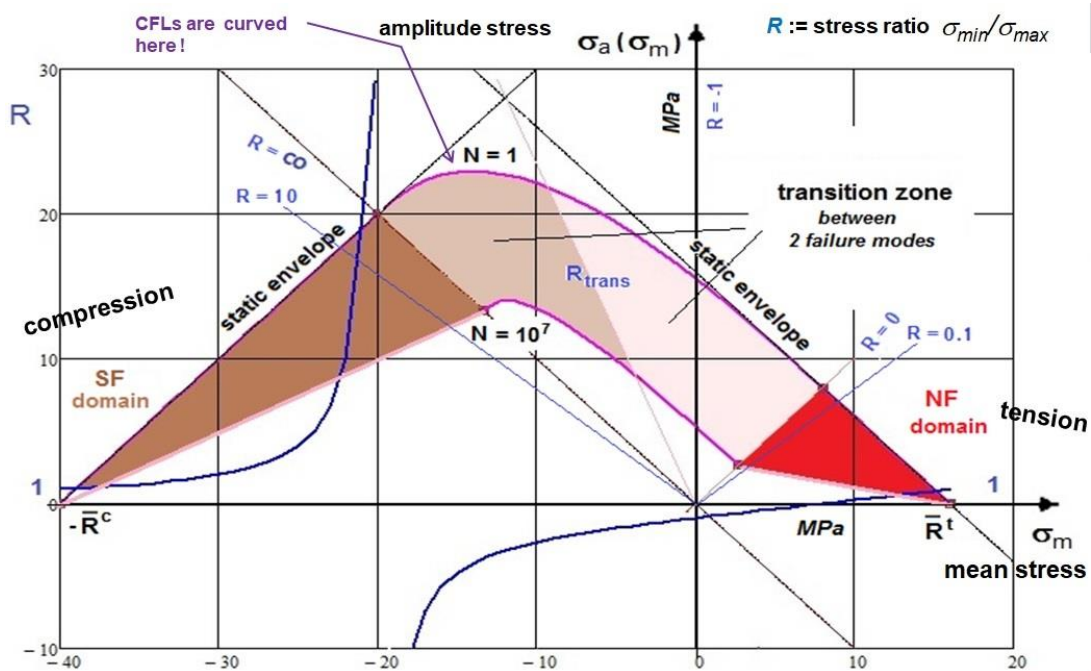


*Fig.11: Scheme of pure mode domains, course of R and transition zone parts*

The CFL curve  $N = 1$  is curved at top because 2 modes act in the case of brittle materials. This is in contrast to uniaxial static loading, depicted by the straight static envelopes.  $N \neq N_f$ . One micro-damage cycle results from the sum of 2 micro-damage portions, one comes from uploading and one from unloading!

*(The associated MathCad program, which involves test data evaluation, parameter determination of Weibull curves, of Master curves, of decay functions, computation operations and visualization afforded more than 30 pages).*

The full procedure is collected in the [Table 8](#). Here, and this is reasonable for brittle materials, all the SN curves have their origin in the strength points  $\bar{R}^t$  and  $\bar{R}^c$ .

Table 8: Full procedure of the automatic determination of a CFL curve. IFF, N=105 cycles

1 Choice of the distinct CFL (example N =10<sup>5</sup>)

2 Determination of the 2 Master curves

Assumption: usual test curves R=0.1 (NF), R=10 (SF) are sufficient instead of R=0, R=1000  $\cong \infty$

$$\sigma_{max}^{Master}(N, R = 0.1) \rightarrow = \sigma_{R=0.1} = c_1^{NF} + (\bar{R}^t - c_1^{NF}) / \exp\left(\frac{\log(N)}{c_1^{NF}}\right)^{c_2^{NF}}$$

$$\sigma_{min}^{Master}(N, R = 10) \rightarrow = \sigma_{R=10} = c_1^{SF} + (-\bar{R}^c - c_1^{SF}) / \exp\left(\frac{\log(N)}{c_1^{SF}}\right)^{c_2^{SF}} .$$

3 Assumption: Straight asymptotic side lines in the 2 mode domains  $\sigma_a(\sigma_m) = c_1 + c_2 \cdot \sigma_m$

2 strength points are given and 2 mean  $\sigma_a(\sigma_m, N)$  of R=0.1 and R=10 are to compute

as a fixed point of each side line

4 Computation of the fixed points in the domains NF, SF (n MPa )

$$\sigma_{R=0.1}^{100000} = 27.3 \rightarrow \sigma_{aR=0.1}^{100000} = 0.5 \cdot \sigma_{R=0.1}^{100000} \cdot (1-0.1) = 12.3, \quad \sigma_{mR=0.1}^{100000} = \sigma_{R=0.1}^{100000} - \sigma_{aR=0.1}^{100000} = 15.0,$$

$$\sigma_{R=10}^{100000} = -136.5 \rightarrow \sigma_{aR=10}^{100000} = -0.5 \cdot \sigma_{R=10}^{100000} \cdot (1-1/10) = 61.4, \quad \sigma_{mR=10}^{100000} = \sigma_{R=10}^{100000} + \sigma_{aR=10}^{100000} = -75.$$

5 Function for the decay of mode influences  $\sigma_a(\sigma_m)$  over the transition zone

Parameters sets from the strength point and a fixed point  $f_d = 1 / [1 + \exp((c_1 + \sigma_m)/c_2)]$ .

$$f_d(\text{SF}): (\sigma_a, \sigma_m, N, R=10) \rightarrow 0.99 \text{ with } (\sigma_a, \sigma_m, N, R=0.1) \rightarrow 0.01 ;$$

$$f_d(\text{NF}): (\sigma_a, \sigma_m, N, R=10) \rightarrow 0.01 \text{ with } (\sigma_a, \sigma_m, N, R=0.1) \rightarrow 0.99.$$

6 'Static' envelope curve: Solving the interaction equation for  $\sigma_a(\sigma_m, N = 1)$

$$\left(\frac{-(\sigma_{2m} - \sigma_{2a}) + |\sigma_{2m} - \sigma_{2a}|}{2 \cdot \bar{R}_\perp^c}\right)^m + \left(\frac{\sigma_{2m} + \sigma_{2a} + |\sigma_{2m} + \sigma_{2a}|}{2 \cdot \bar{R}_\perp^t}\right)^m = 1 \rightarrow \sigma_{2a}(\sigma_{2m}, \bar{R}_\perp^c, \bar{R}_\perp^t).$$

7 Asymptotic side line approach for the decaying curves  $\sigma_a(\sigma_m, N > 1)$

$$[\sigma_{2a}(\sigma_{2m}, N)]^m = (c_{1SF} + c_{2SF} \cdot \sigma_{2m})^m + (c_{1NF} + c_{2NF} \cdot \sigma_{2m})^m$$

Work case N = 10<sup>5</sup> cycles, m = 2.5

$$c_{1SF} = 0.63 = c_{2SF}, \quad c_{1NF} = 0.34 = -c_{2NF}; \quad c_{1SF5} = -40.6, \quad c_{2SF5} = -5.56, \quad c_{1NF5} = -49.5, \quad c_{2NF5} = 5.55$$

$$\sigma_{2a}(\sigma_{2m}, N=10^5, c_i) = \left[ \left( \frac{c_{1SF} + c_{2SF} \cdot \sigma_{2m}}{1 + \exp\left(\frac{c_{1SF5} + \sigma_{2m}}{c_{2SF5}}\right)} \right)^m + \left( \frac{c_{1NF} + c_{2NF} \cdot \sigma_{2m}}{1 + \exp\left(\frac{c_{1NF5} + \sigma_{2m}}{c_{2NF5}}\right)} \right)^m \right]^{1/m} .$$

The following points are to consider thereby:

- Assumption: "If the failure mechanism of a mode cyclically remains the same as in the brittle static case, then the micro-damage-driving fatigue failure parameters are

the same and the applicability of static SFCs is allowed for quantifying micro-damage portions“

- Presumption: An appropriate Master SN curve for each failure mode domain compression (SF) and tension (NF) is available at minimum. This means measurement of just a minimum number of SN curves is required
- The helpful model, searched by the author, became the ‘Modified Fatigue Strength Ratio  $\Psi$  model’ of Kawai [16], which enables to estimate SN curves. Kawai captures all SN curves in tension (NF) and in compression (SF) domain by one  $\Psi$  and then he determines also SN curves in the transition zone around  $R_{trans}$ . The boundary R-curves are automatically captured by the model
- According to his modal FMC thinking Cuntze dedicated a  $\Psi$  to each single failure modes domain SF and NF. Other necessary SN curves, necessary for the verification of the usually faced variable amplitude operational loading, can then be derived from the mode Master SN curve.
- Cuntze separates the mode regimes to stay in the mode domains better physically-based. However, then he needs above mentioned decay function  $f_{decay} = 1 / (1 + exp(c1 + \sigma_m / c2))$  in both the domains to make the determination of SN curves and of CFL curves in the transition zone possible.
- A quality check of the two approaches is possible if enough SN curves, distributed over the full Haigh diagram, will be available in literature for a material with a large strength ratio.

## 5.2 CFL curves, applying the Mode Decay Functions $f_d$ in various UD Haigh-Diagrams

### 5.2.1 FF SN curves and associate Haigh Diagram

Some examples of SN-curves, ‘feeding’ the associated Haigh-Diagrams, are presented. These belong to the failures FF and IFF and capture the failure types NF (tension) and SF (compression).

In [Fig.12](#) FF-test data from Kawai-Suda [16] are depicted and mapped by the four parameter Weibull approach. [Fig.12](#) gives a feeling how the bulk of measured SN curves usually looks.

It further shows how the mapped curves are running in the higher VHCF regime. There is no fidelity given when using extrapolated values far off the tested range.

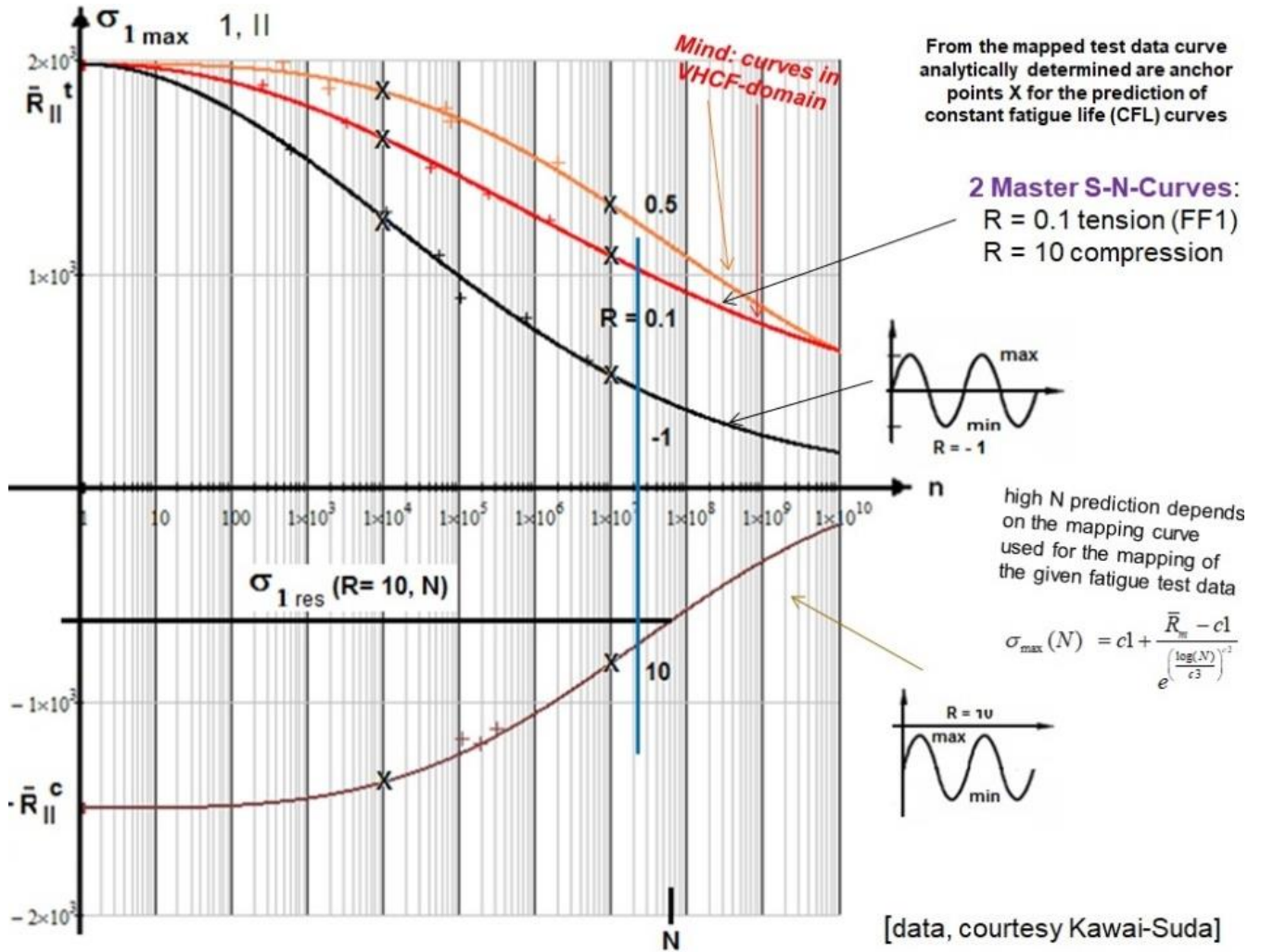


Fig.12, Test example UD: Individually lin-log mapped FF1-FF2-linked SN-curves [16]

Fig.13 presents failure mode-linked CFL-curves  $\sigma_a$  ( $\sigma_m$ ,  $N = \text{constant}$ ). The computed SN curve points, marked by X, are fixed points (anchors) for mapping the CFL curves to be predicted. The blue curve is for  $N = 10^5$  cycles. The used SN-curves are from Fig.12.



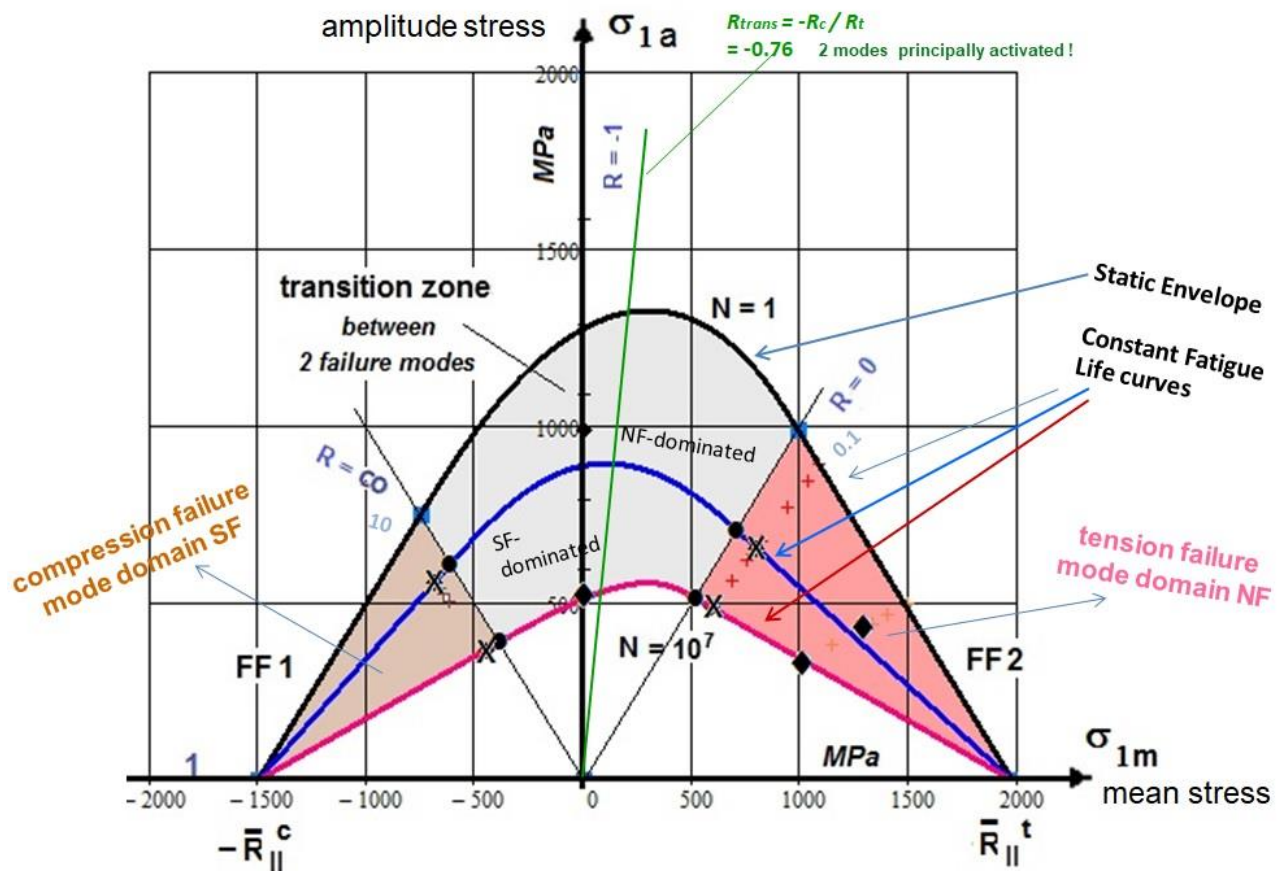


Fig.13: Rigorous Interpretation of the Haigh diagram for the UD-example FF1-FF2 displaying failure mode domains and transition zone [16]

CFRP/EP,  $\bar{R}_{II}^t = 1980$ ,  $\bar{R}_{II}^c = 1500$ ,  $\bar{R}_{\perp}^t = 51$ ,  $\bar{R}_{\perp}^c = 172$ ,  $\bar{R}_{\perp||} = 71$  [MPa].

### 5.2.2 IFF3 SN curves and associate Haigh Diagram

Fig.14 presents two mapped IFF3 SN curves.

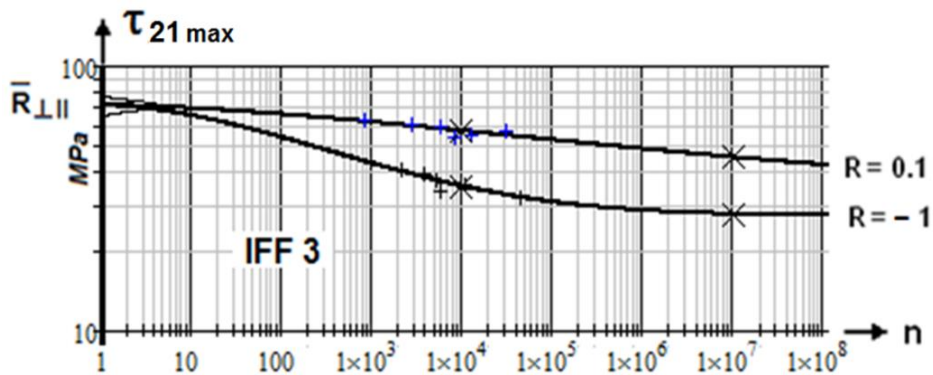
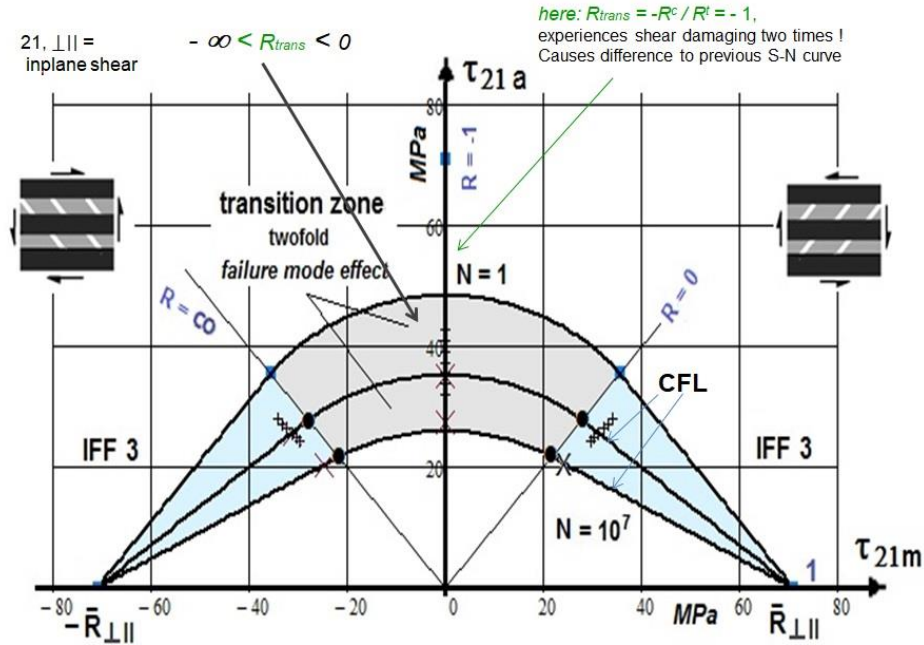


Fig.14: Log-log IFF3-linked SN curves (data, courtesy C. Hahne, [15])

Here, at first the author likes to thank Dr.-Ing. Clemens Hahne, AUDI, for his valuable UD test effort making the generation of the following figures possible and thereby the application of the

author's CFL model. The reader is invited to read the content-rich and imaginative dissertation [15] and this not only for comparing the different CFL modeling ideas of Hahne and Cuntze.

*Fig.15* depicts the associated IFF3 CFL curves derived. Obvious is the symmetry and that the two-fold mode micro-damage effect flattens the curve at  $\sigma_m = 0$ .



*Fig.15: IFF3 UD Haigh diagram, Display of a two-fold mode effect ( $a :=$  amplitude,  $m :=$  mean,  $N :=$  number of fracture cycles,  $\bar{R} :=$  strength and  $R := \sigma_{min}/\sigma_{max}$ ). Test data CF/EP, courtesy Hahne [15]*

### 5.2.3 IFF1, IFF2 SN-curves and associated Haigh Diagram

In *Fig.16* the mapped IFF1 (tension)- and IFF2 (compression)-linked SN-curves are presented.

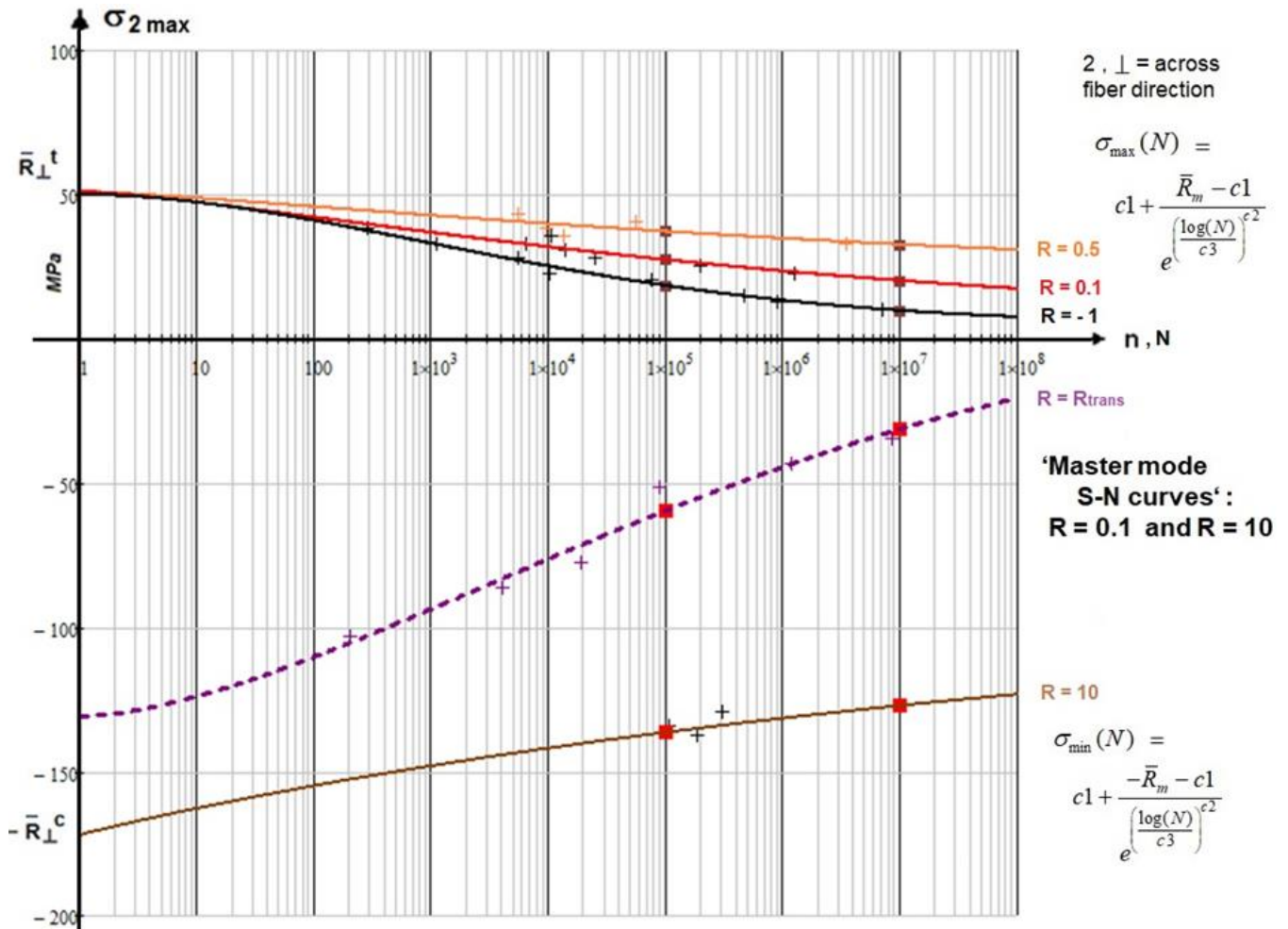


Fig.16: Mapped lin-log IFF1-IFF2-linked SN curves [test data, courtesy C. Hahne]

Fig.17 displays the differently colored failure mode domains IFF1-IFF2 in a UD IFF Haigh diagram. The available test data set along  $R_{\text{trans}}$  in the transition zone is represented by the crosses.

The decay model quality in Fig.17 proves the efficiency of the decay functions in the transition zone. For proving this the author is very thankful because this was only possible because he got access to the test results in [15]).

By the way:

The decaying course of the curve in the graph below for UD material is similar to concrete due to their large strength ratios  $R^c / R^t$  ! Similar behavior permits similar description!

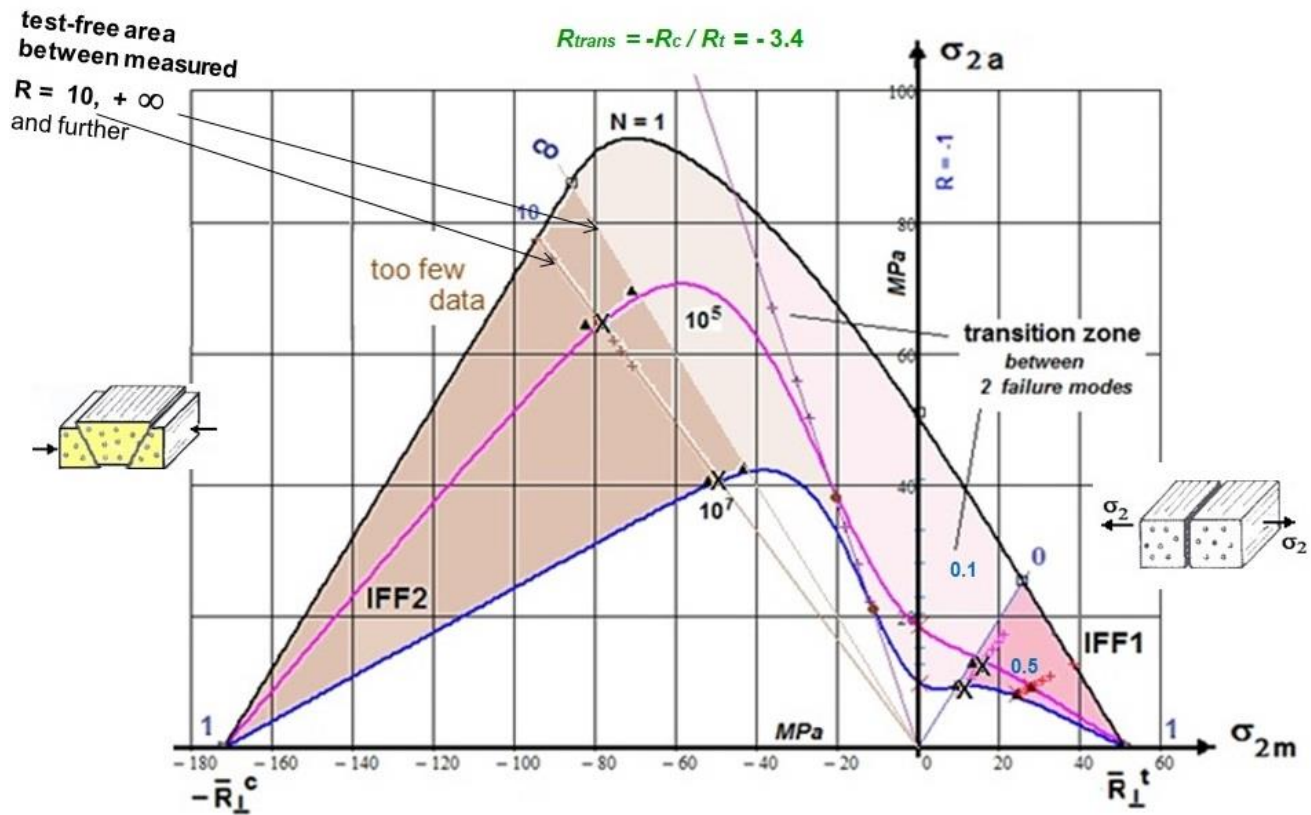


Fig.17: IFF1- IFF2 UD Haigh diagram (similar for UD, lamella and concrete) displaying the failure mode domains, transition zone [15]

### 5.3 Steps of the FMC-based Fatigue Life Estimation Procedure

The steps of the fatigue life estimation procedure are depicted in the following figures. **Step 1** is searching measured SN curves. Fig.18 presents a measured SN-curve that serves as master SN curve. This SN curve can be mapped here by a straight line in a log-log diagram.

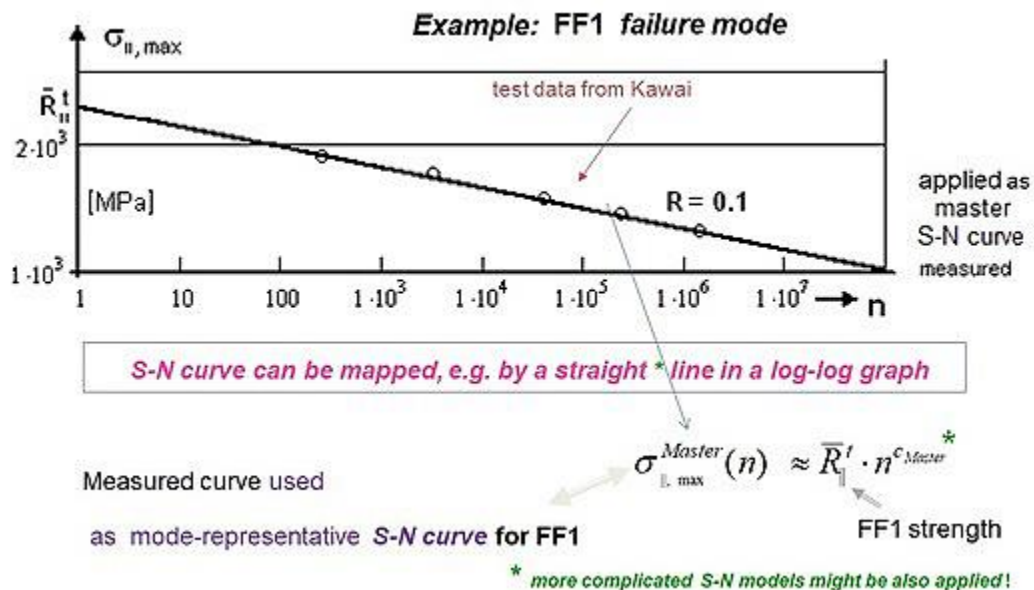


Fig.18: Mapping of UD FF1 SN data and mode-representative Master SN curve

In the case of variable amplitude loading several SN curves are needed. This will be performed exemplarily for the tension domain FF1 in Fig.19 by application of Kawai's  $\Psi$  model, however here by a mode-wise application.

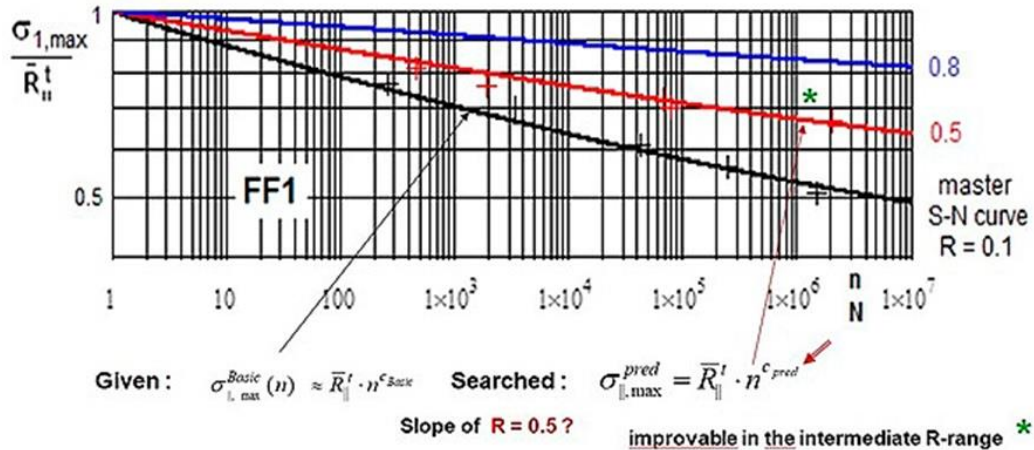


Fig.19: Prediction of other needed FF1 SN curves from Master mode SN curve and Cuntze's mode-dedicated Kawai model ( $\Psi$  curve)

Statistical analyses have shown that the fatigue life estimation using the linear accumulation method of Palmgren-Miner tends to be too optimistic, Fig.20. However a satisfactory reason could not yet found. One explanation is the 'right use of the right SFC'. A more severe explanation is the loss of the loading sequence which is different for ductile and brittle materials. This is practically considered in design by the application of the Relative Miner with a  $D_{feasible} < 100\%$ .

Note on UD material:

Dependent on the lay-up, the length of individual fiber and on the chosen matrix the fatigue resistance comes to act. 'Well-designed' (*optimal fiber directions and minimum amount of fiber reinforcement for all load cases*) high-performance UD lamina-composed laminates are less endangered. Concerning the mode-representative Master SN-curves: These should be derived from sub-lamina test specimen results, which capture the embedding (in-situ) effects.

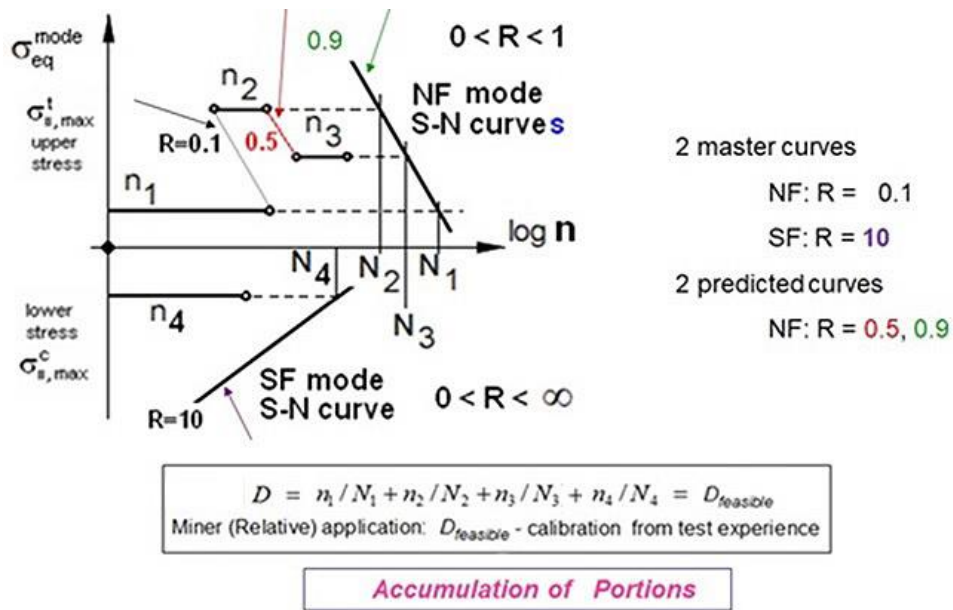


Fig.20: Lifetime Prediction (estimation) Method.  
Schematic application of a simple example, 4 blocks.  $D_{feasible}$  from test experience derived

Fig.21 finally shall briefly give the fatigue life estimation procedure for the example laminate. Due to the lack of test data regarding ductile and slightly brittle metals the author could not generally apply the CFL generation method above.

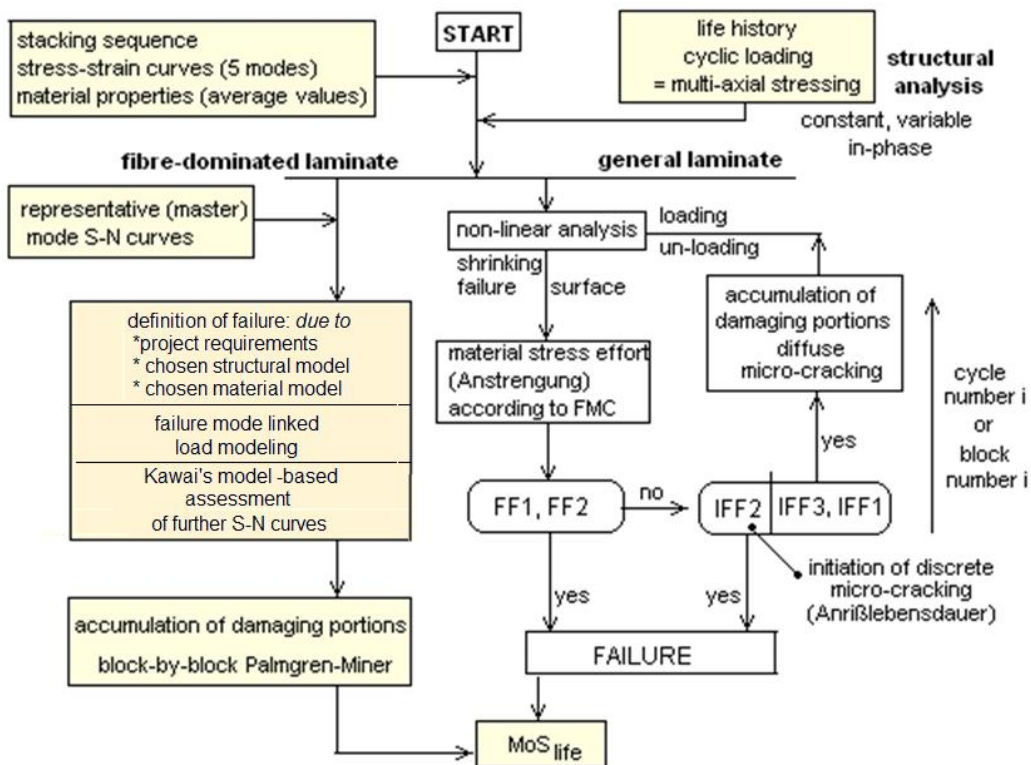


Fig.21: Non-linear estimation of a laminate's fatigue life

## 6 Conclusions on the Elaborated Novel Ideas

Novel simulation-driven product development shifts the role of physical testing to virtual testing. This requires High Fidelity concerning the material models used, such as the static strength criteria (SFC) and the lifetime estimation criteria. Based on his FMC ideas the author successfully derived static SFCs for a large variety of isotropic brittle structural materials such as plexiglass, porous concrete stone, cast iron, Normal Concrete, UHPC sandstone, mild steels, foam, monolithic ceramics and for the transversely-isotropic UD fiber-reinforced polymers Lamina (ply, lamella) and orthotropic ceramic Fabrics. Available multi-axial fracture test data for above materials data were mapped to validate the SFCs. Practical experience showed, that for brittle materials these static SFCs are applicable to quantify the micro-damage portions under cyclic loading.

Basic idea in this paper was the generation of automatically derived, numerically constructed Constant Fatigue Life (CFL) curves using just one SN Master curve for each mode, at minimum. The author was only able to realize this when he became aware of a general SN curve modeling method, namely Kawai's  $\Psi$  method, which was physically better based than the predecessors used by the author. This  $\Psi$  method the author used in each mode domain separately, due to his strict failure mode thinking.

Challenging was the description of the R-beams in the transition zone between the tension and the compression mode domain, where a huge decay of the CFL curve is faced from the compression domain down to the tension domain if the strength ratio is high. Therefore, a physically-based decay function has been applied to describe this. In addition, in contrast to the mode domain-linked SN-beams, the static origin point of a R-beam in the transition zone, which represents a mixed failure domain, was especially to determine to obtain a beam description.

The application of the presented procedure was successful in several UD Haigh Diagrams and invites for more investigation. Hopefully, the author has posted to the industrial and the university reader a message which is understandable, concise and memorable to let them convincingly search for the necessary research funding.

With this document, the author attempts to redirect the thinking resulting from ductile material behavior in 'Mean stress influence' into thinking with fracture modes of brittle materials. If pretty ductile one has one mode 'yielding' and if pretty brittle many modes 'fracture'.

The final Table gives a survey on essential points of the various Haigh Diagrams faced with isotropic and transversely-isotropic UD materials.

Table: Haigh Diagram Essentials of isotropic and transversely-isotropic materials

ductile	<b>Isotropic material</b>	brittle
$R = R_{0.2}^t$	$\{\sigma\} = (\sigma_I, \sigma_{II}, \sigma_{III})^T$	$\{R\} = (R^t, R^c, )^T$ with $\mu$
1 mode yielding	2 fracture modes	
1 yield mode domain	2 fracture mode domains with transition zone	
<i>Increasing 'Mean stress influence' with increasing strength ratio number <math>R^c/R^t</math></i>		

Interaction of *stresses* by Strength Failure Criteria (SFC)

1 SFC ('Mises') yield failure mode	2 SFCs, fracture failure modes, NF +SF
$Eff^{yield\ mode} = \frac{\sigma_{eq}^{Mises}}{R_{0.2}^t} / R_{0.2}$	$\Leftrightarrow Eff^{fracture\ mode} = \frac{\sigma_{eq}^{fracture\ mode}}{\sigma_{eq}^{fracture\ mode}} / R$

Interaction of *failure modes* for determination of 'Onset-of-failure' by an interaction equation

$$Eff = \frac{\sqrt{3J_2}}{R_{0.2}^t} = \frac{\sigma_{eq}^{Mises}}{R_{0.2}^t} = 1 = 100\% \quad \Leftrightarrow \quad Eff = \sqrt[m]{(Eff^{mode\ 1})^m + (Eff^{mode\ 2})^m} = 1$$

1 Haigh Diagram required.

**Transversely-isotropic UD material, brittle (no edge effect)**

$$\{\sigma\} = (\sigma_1, \sigma_2, \sigma_3, \tau_{23}, \tau_{31}, \tau_{21})^T \quad \Leftrightarrow \quad \{R\} = (R_{||}^t, R_{||}^c, R_{\perp}^t, R_{\perp}^c, R_{\perp||})^T \quad \text{with } \mu_{\perp||}, \mu_{\perp\perp}$$

$$\{\sigma_{eq}^{mode}\} = (\sigma_{eq}^{||\sigma}, \sigma_{eq}^{||\tau}, \sigma_{eq}^{\perp\sigma}, \sigma_{eq}^{\perp\tau}, \sigma_{eq}^{||\perp})^T \quad 5 \text{ fracture modes}$$

$$\text{FF1: } Eff^{||\sigma} = \check{\sigma}_1 / \bar{R}_{||}^t = \sigma_{eq}^{||\sigma} / \bar{R}_{||}^t \quad \text{with } \check{\sigma}_1 \cong \varepsilon_1^t \cdot E_{||} \text{ (matrix neglected)}$$

$$\text{FF2: } Eff^{||\tau} = -\check{\sigma}_1 / \bar{R}_{||}^c = +\sigma_{eq}^{||\tau} / \bar{R}_{||}^c \quad \text{with } \check{\sigma}_1 \cong \varepsilon_1^c \cdot E_{||}$$

$$\text{IFF1: } Eff^{\perp\sigma} = [(\sigma_2 + \sigma_3) + \sqrt{\sigma_2^2 - 2\sigma_2 \cdot \sigma_3 + \sigma_3^2 + 4\tau_{23}^2}] / 2\bar{R}_{\perp}^t = \sigma_{eq}^{\perp\sigma} / \bar{R}_{\perp}^t$$

$$\text{IFF2: } Eff^{\perp\tau} = [a_{\perp\perp} \cdot (\sigma_2 + \sigma_3) + b_{\perp\perp} \sqrt{\sigma_2^2 - 2\sigma_2 \sigma_3 + \sigma_3^2 + 4\tau_{23}^2}] / \bar{R}_{\perp}^c = \sigma_{eq}^{\perp\tau} / \bar{R}_{\perp}^c$$

$$\text{IFF3: } Eff^{\perp||} = \{[2 \cdot \mu_{\perp||} \cdot I_{23-5} + (\sqrt{b_{\perp||}^2 \cdot I_{23-5}^2 + 4 \cdot \bar{R}_{\perp||}^2 \cdot (\tau_{31}^2 + \tau_{21}^2)^2}] / (2 \cdot \bar{R}_{\perp||}^3)\}^{0.5} = \sigma_{eq}^{\perp||} / \bar{R}_{\perp||}$$

$$\text{with } a_{\perp\perp} \cong \mu_{\perp\perp} / (1 - \mu_{\perp\perp}), \quad b_{\perp\perp} = a_{\perp\perp} + 1, \quad I_{23-5} = 2\sigma_2 \cdot \tau_{21}^2 + 2\sigma_3 \cdot \tau_{31}^2 + 4\tau_{23}\tau_{31}\tau_{21}$$

Consequently, the FMC-approach requires an interaction of all modes which reads

$$Eff = \sqrt[m]{(Eff^{mode\ 1})^m + (Eff^{mode\ 2})^m + \dots + \dots + \dots} = 1 = 100\% \quad \text{for Onset-of-Failure.}$$

3 Haigh Diagrams required: FF1 with FF2, IFF1 with IFF2 and IFF3.

2D: Max and min (mathem.) UD-lamina stresses replace the principal stresses of isotropic materials.

3D: Idea. The absolute UD-equivalent stress values replace the single UD-lamina stresses in order to capture a 3D stress state including the delamination-causing fatigue-relevant inter-laminar stresses (index 3). NF-linked-equivalent mode stresses are placed on the positive Haigh abscissa.



## REFERENCES

1. R. Cuntze, “Life-Work *Cuntze* - a compilation”, > 750 pages, Draft February 2023, permanent downloading address from [Carbon Connected | Prof. Ralf Cuntze \(carbon-connected.de\)](https://www.carbon-connected.de/)
2. R. Cuntze, “Application of 3D-strength criteria, based on the so-called “Failure Mode Concept”, to multi-axial test data of sandwich foam, concrete, epoxy, CFRP-UD lamina, CMC-Fabric Lamina”, ICCE/5, Las Vegas, July 1998 (presentation)
3. R. Cuntze, “Failure Conditions for Isotropic Materials, Unidirectional Composites, Woven Fabrics - their Visualization and Links”, <https://www.ndt.net › cdc2006 › papers › cuntze, PDF>
4. R. Cuntze, “Fracture Failure Bodies of Porous Concrete (foam-like), Normal Concrete, Ultra-High-Performance-Concrete and of the Lamella - generated on basis of Cuntze’s Failure-Mode-Concept (FMC)”. NWC2017, June 11-14, NAFEMS, Stockholm
5. R. Cuntze, “Strength Failure Conditions of the Various Structural Materials: Is there some Common Basis existing?, SDHM, vol.074, no.1, pp.1-19, 2008
6. R. Cuntze, “Static & Fatigue Failure of UD-Ply-laminated Parts – a personal view and more”. ESI Group, Composites Expert Seminar, Technical University Stuttgart, January 2015, keynote presentation
7. HSB “Handbuch Struktur Berechnung (in English) – German Aeronautical Handbook - Fundamentals and Methods for Aeronautical Design and Analyses”. Editor is the IASB working group (*the author was active member from 1972-2016*)
8. German Guideline, Sheet 3, “Development of Fibre-Reinforced Plastic Components, Analysis”, [Beuth-Verlag](https://www.beuth-verlag.de/), 2006 (in German and English, author was convenor and co-author)
9. B. Pyttel, D. Schwerdt and C. Berger, “Very high cycle fatigue – Is there a fatigue limit?” In Intern. J. Fatigue (33), 2011, 1, pp. 49–58:
10. S.W. Tsai and E. M. Wu, “A General Theory of Strength for An-isotropic Materials”, Journal Comp. Materials 5 (1971), 58-80
11. R. Cuntze: “Technical terms for composite components in civil engineering and mechanical engineering. Fachbegriffe mit Erklärung und Definition“. In: Fachbegriffe für Kompositbauteile – Technical terms for composite parts. Springer Vieweg, Wiesbaden, 2019, 171 pages
12. H. Awaji and S. Sato, “A Statistical Theory for the Fracture of Brittle Solids under Multiaxial Stresses”. Int. J. of Fracture, 14 (1978), R 13-16
13. R. Cuntze, “Comparison between Experimental and Theoretical Results using Cuntze’s Failure Mode Concept model for Composites under Tri-axial Loadings – Part B of the WWFE-II. Journal of Composite Materials”, Vol.47 (2013), 893-924
14. A. Puck, „Festigkeitsanalyse von Faser-Matrix-Laminaten - Modelle für die Praxis“, München, Carl Hanser Verlag, 1996

15. C. Hahne, „Zur Festigkeitsbewertung von Strukturbauteilen aus Kohlenstofffaser-Kunststoff-Verbunden unter PKW-Betriebslasten“, Shaker Verlag, Dissertation 2015, TU-Darmstadt, Schriftenreihe Konstruktiver Leichtbau mit Faser-Kunststoff-Verbunden, Herausgeber Prof. Dr.-Ing Helmut Schürmann
16. M. Kawai, “A phenomenological model for off-axis fatigue behavior of uni-directional polymer matrix composites under different stress ratios”, Composites Part A 35 (2004), 955-963

**Acknowledgement:**

Above single authored elaboration includes works that have been performed by the author in his vacant time. In this context, many thanks to Wilfried, who believed in me and my Failure-Mode-Concept, which is also the central base for the Constant-Fatigue-Life curve procedure above. Further the author is grateful for the provision of UD test data from Clemens Hahne, AUDI, and for the remarks of Holger Hicketier, Airbus, to an old draft of this elaboration.

The elaboration of the author’s different ideas and their visualizations were not funded. Highest funding would be to obtain valuable comments and critics from colleagues from academia and industry.